

Stephen F. Austin State University

SFA ScholarWorks

Electronic Theses and Dissertations

Spring 5-6-2023

Characterization of Molecular Content, Cytotoxicity, and Anti-Inflammatory Activity of Extractions from Eupatorium serotinum

Jordy Sloan

sloanjm1@jacks.sfasu.edu

Follow this and additional works at: <https://scholarworks.sfasu.edu/etds>



Part of the [Biology Commons](#)

[Tell us](#) how this article helped you.

Repository Citation

Sloan, Jordy, "Characterization of Molecular Content, Cytotoxicity, and Anti-Inflammatory Activity of Extractions from Eupatorium serotinum" (2023). *Electronic Theses and Dissertations*. 494.

<https://scholarworks.sfasu.edu/etds/494>

This Thesis is brought to you for free and open access by SFA ScholarWorks. It has been accepted for inclusion in Electronic Theses and Dissertations by an authorized administrator of SFA ScholarWorks. For more information, please contact cdsscholarworks@sfasu.edu.

Characterization of Molecular Content, Cytotoxicity, and Anti-Inflammatory Activity of Extractions from *Eupatorium serotinum*

Creative Commons License



This work is licensed under a [Creative Commons Attribution-Noncommercial-No Derivative Works 4.0 License](https://creativecommons.org/licenses/by-nc-nd/4.0/).

**Characterization of Molecular Content, Cytotoxicity, and Anti-
Inflammatory Activity of Extractions from *Eupatorium serotinum***

By

JORDAN MONROE SLOAN, B.S. in Genetics

Presented to the Faculty of the Graduate School of

Stephen F. Austin State University

In Partial Fulfillment

Of the Requirements

For the Degree of

Master of Science

STEPHEN F. AUSTIN STATE UNIVERSITY

May, 2023

**Characterization of Molecular Content, Cytotoxicity, and Anti-
Inflammatory Activity of Extractions from *Eupatorium serotinum***

By

JORDAN MONROE SLOAN, B.S. in Genetics

APPROVED:

Dr. Robert Wiggers, Thesis Director

Dr. Darrell Fry, Committee Member

Dr. Karol Chandler-Ezell, Committee Member

Dr. Matthew Kwiatkowski, Committee Member

Sheryll Jerez, Ph.D.
Interim Dean of Research and Graduate Studies

ABSTRACT

Inflammation is a complex and varied immune response which can be expressed chronically or as a temporary reaction to foreign invaders. Symptoms of inflammation include swelling, pain, soreness, and difficulty of motion. Recently, the effect of sesquiterpene lactones such as Helenalin from *Arnica montana* have been studied for their anti-inflammatory properties. In this study, we identified and harvested samples of *Eupatorium serotinum*, a plant historically used by Native Americans to treat a variety of medical illnesses. Crude extracts of the leaves, flowers, roots, and stems were prepared by ethanol extraction. The cytotoxicity of the different extracts on HEK293 cells was determined by a cell death assay and a cell viability assay. HPLC was performed on the extracts and compared with a Helenalin standard to determine the possible presence of sesquiterpene lactones isolated from *E. serotinum*. Finally, an inflammation assay was performed on TNF- α stimulated HEK293 cells pretreated with the extract, and the total RNA was extracted and sequenced to study the differential gene expression.

ACKNOWLEDGEMENTS

Firstly, I would like to thank the Department of Biology and the Department of Chemistry who provided funding for this project despite the short notice. I would like to thank my thesis advisor Dr. Robert Wiggers for guiding me through the data collection and thesis defense process, as well as Dr. Donald Pratt who was my original advisor throughout the proposal process. I also have to express my deepest appreciation to Dr. Darrell Fry for his support on the chemical analyses and project planning. I would also like to thank Dr. Karol Chandler-Ezell for her guidance during the inception of the project as well as her knowledge of ethnobotany and plant handling. Dr. Kwiatkowski was also very helpful throughout the project by helping me with the planning and logistics of this thesis. Also, I would like to give my thanks to my grandparents John and Kay Sloan, who's support and encouragement was vital to the completion of this research, and who helped me search for and identify *Eupatorium serotinum* near their home. I would also like to thank my grandmother Mattie Kathleen Benjamin for her motivation and wisdom which have been crucial to my education. Finally, I would like to extend my sincere thanks to my parents, John Gilbert King Sloan and Marilyn Rene Muhm Sloan for their love and encouragement.

TABLE OF CONTENTS

ABSTRACT	i
ACKNOWLEDGEMENTS	ii
TABLE OF CONTENTS	iii
List of Figures	vi
List of Tables	viii
INTRODUCTION	1
Traditional and Folk Medicine Overview	1
Traditional and Folk Medicine for Inflammation	3
<i>Arnica montana</i>	4
<i>Eupatorium serotinum</i>	6
Project Overview	10
Inflammation Pathway	11
Anti Inflammatory Drugs and Sesquiterpene Lactones	14
High Performance Liquid Chromatography	15
Human Cell Culturing	17
HEK293 Cells	20

Cytotoxicity Testing	21
Differential Expression Analysis	22
MATERIALS AND METHODS.....	27
Field Collection of Eupatorium Serotinum	27
Preparation of Herbarium Voucher Specimen.....	28
Crude Ethanol Extraction	29
HEK-293 Cell Culturing	30
Toxicity Testing - Cell Death Assay.....	31
Toxicity Testing - Cell Viability Assay.....	33
Mycoplasma Contamination Testing	33
Inflammation Assay.....	34
RNA Extraction.....	34
Transcriptomic Analysis	35
HPLC.....	36
RESULTS AND DISCUSSION	37
Plant Collection and Herbarium Voucher	37
HEK293 Growth and Mycoplasma Contamination	41
Cytotoxicity of Extractions	42

HPLC for Sesquiterpene Lactone Identification.....	51
Inflammation Assay and Differential Gene Expression.....	61
CONCLUSION.....	71
REFERENCES.....	76
VITA	85

List of Figures

Figure 1. <i>Eupatorium serotinum</i> Distribution - Biota of North America Program (BONAP)	8
Figure 2. <i>Eupatorium serotinum</i> - University of Southern Florida, Institute for Systematic Botany.....	9
Figure 3. Mycoplasma Contamination Testing with Hoechst Dye.....	20
Figure 4. <i>Eupatorium serotinum</i> harvested from Holly Lake Ranch.....	38
Figure 5. <i>Eupatorium serotinum</i> herbarium voucher specimen	39
Figure 6. <i>E. serotinum</i> ethanol extraction jars	40
Figure 7. Mycoplasma contamination testing of HEK293 Cells	42
Figure 8. Cell Death Assay - Ethanol Extract	44
Figure 9. Cell Death Assay - PBS Extract	45
Figure 10. Cell Viability Assay - Ethanol Extract.....	46
Figure 11. Cell Viability Assay - PBS Extract.....	47
Figure 12. Cell Viability Assay - Leaf Extract.....	48
Figure 13. Cell Viability Assay - Stem Extract.....	49
Figure 14. Cell Viability Assay - Flower Extract	50
Figure 15. Cell Viability Assay - Root Extract	51
Figure 16. HPLC Chromatogram - PBS Extract.....	54

Figure 17. HPLC Chromatogram - Ethanol Extract.....	55
Figure 18. HPLC Chromatogram - Leaf Extract.....	56
Figure 19. HPLC Chromatogram - Stem Extract	57
Figure 20. HPLC Chromatogram - Flower Extract	58
Figure 21. HPLC Chromatogram - Root Extract	59
Figure 22. HPLC Chromatogram - Helenalin Standard	60
Figure 23. HPLC Chromatogram - Comparative Absorbance Spectra of RT 17 Peak	61
Figure 24. Volcano plot PBS extract vs. Control.....	63
Figure 25. Volcano plot TNF- α vs. Control	65
Figure 26. Volcano plot PBS extract / TNF- α vs. Control.....	67
Figure 27. Volcano plot PBS extract / TNF- α vs. TNF- α treatment.....	69

List of Tables

Table 1. HPLC Chromatogram Peaks - PBS Extract.....	54
Table 2. HPLC Chromatogram Peaks - Ethanol Extract.....	55
Table 3. HPLC Chromatogram Peaks - Leaf Extract	56
Table 4. HPLC Chromatogram Peaks - Stem Extract.....	57
Table 5. HPLC Chromatogram Peaks - Flower Extract	58
Table 6. HPLC Chromatogram Peaks - Root Extract	59
Table 7. HPLC Chromatogram Peaks - Helenalin Standard.....	60
Table 8. Differentially Expressed genes for PBS Extract vs. Control.....	64
Table 9. Differentially expressed genes for TNF- α vs. Control	66
Table 10. Differentially expressed genes for PBS Extract / TNF- α vs. Control..	68
Table 11. Differentially expressed genes for PBS extract vs. TNF- α treatment..	70

INTRODUCTION

Traditional and Folk Medicine Overview

Before the adoption of modern western medicine, most ailments were treated with folk and traditional medicine, also called ethnomedicine.

Ethnomedicine medicine refers to the healing practices that have been passed down through centuries. These practices are not often uniform, and can vary depending on the specific region, culture, or the population's access to different plants, animals, or minerals (1). Folk and traditional remedies are still employed in a variety of areas, from rural towns to large urban centers. One large subset of traditional medicine is Traditional Chinese Medicine which has been the focus of considerable study in biomedicine for its ability to treat a variety of medical problems from stroke and heart disease to mental disorders. In fact, a recent survey in the U.S. shows that as many as 20% of Americans use a traditional Chinese herbal product (2).

North America has a rich history with traditional folk medicine, both from the thousands of years of indigenous American use, and from the more recent imports from early European settlers. Despite the long history of these traditions among indigenous cultures, Native American communities are facing major challenges in preserving this cultural knowledge. Recently, efforts have been

made to integrate some aspects of traditional medicine with the modern western healthcare system (3).

One of the main challenges in the preservation of traditional medicine is the lack of proper scientific interest and study in the folk remedies that have been used by local people for centuries. Modern pharmaceutical research and development often requires decades of study to determine the chemical properties of a compound, the mechanism of actions, toxicity, off-target effects, and long-term safety of a novel treatment. In fact, due to many possible factors such as the difficult regulatory hurdles, increased cost of clinical trials, and financially driven early project termination; in 2012 FDA approvals for new molecular entity drugs declined by 25% since the 1990s (4). The financial burden as well as the manpower required to satisfy this burden of proof is prohibitive to the study of many local plant species, including such species with a long history of use in folk medicine.

One successful example where scientific investigation of a folk remedy led to drug development comes from Chinese scientists who looked at the chemical composition of *Artemisia annua* (sweet wormwood). Chinese medicine has used sweet wormwood to treat various ailments including malaria and fevers (5). In the 1960s and 1970s, the research team successfully isolated and characterized the compound “artemisinin” from wormwood extracts. This compound would later be

shown to have antimalarial properties, and has been further refined into important antimalarial drugs including artemether and artesunate (6).

Traditional and Folk Medicine for Inflammation

Many folk remedies across the world have been used in the past to fight inflammation related ailments. In Ayurveda (a branch of traditional medicine originating on the Indian subcontinent), turmeric has been used to treat conditions such as arthritis. The active compound, curcumin, has been shown to have anti-inflammatory activity in recent studies (7). Willow bark has been used for thousands of years as a folk remedy for pain. Traditionally, willow bark was brewed into a tea, chewed, or used as a poultice; and contains the compound salicin, an aspirin precursor (8).

The genus *Eupatorium* has been used in the treatment of a variety of inflammation related diseases. *Eupatorium perfoliatum* was used to treat respiratory ailments stemming from colds and viruses, and was often used and sold as a tincture. Tinctures of *E. perfoliatum* have been recognized in medical literature since the late 1800s (9). In South America, *Eupatorium triplinerve* was used in the treatment of inflammation as well as a sedative. Traditionally, it's leaves were used in baths or ingested in a tea (10). *Eupatorium canndinum*, commonly known as hemp agrimony, has also been used as a tea in traditional European medicine to treat digestive diseases (11).

Arnica montana

Arnica montana, is a European flowering plant in the family Asteraceae, order *Asterales*, and Class *Magnoliopsida*. Asteraceae, known commonly as the daisy, aster, or sunflower family, is the largest flowering plant family, composed of over 23,000 species across 1,600 genera. Approximately 300 species of plant from the Asteraceae family are used in Chinese medicine (12). The number of species within the Asteraceae family is comparable only to the *Orchidaceae* family. The study of the Asteraceae family is called “Synantherology,” and current research attempts to more accurately categorize the species in Asteraceae based on evolutionary history and comparative DNA sequencing data (13)

Arnica montana is widely distributed across most of Europe, but is absent from the Italian peninsula and British Isles. The plants grow preferentially in acidic and poor soils, and can be found mainly in grasslands and alpine mountain regions. In some regions the populations are stable, but population decline has been documented in other regions either as a result of plant harvesting for medicinal purposes or due to habitat loss (14). Previous research has identified the eating behaviors of polyphagous herbivores such as mollusks as a limiting factor for the population spread from alpine regions into grasslands (15).

Arnica montana is a perennial plant that flowers from June to July. It has low basal leaves with a bright green color. A fully grown plant will reach approximately 20-60 cm in height. The upper leaves are opposite, spear shaped,

and generally smaller than the lower leaves (16). *Arnica montana* has a thin, hairy stem, and its bright yellow flower is approximately 4.9 to 5.7 cm in diameter. Each plant will bloom with 1-7 flower heads.

As with other members of the *Asteraceae* family, *A. montana* is capable of both vegetative and sexual reproduction. Around June and July, the plant will sexually reproduce through its flowers. It is self-incompatible, a common phenomenon in the *Asteraceae* family, and thus is not able to self-fertilize flowers with pollen from the same plant. Following fertilization, the flowering rosette dies, releasing the seeds as plumed achenes. The seeds (as achenes) are dispersed through the wind, usually in the late summer through autumn, and do not have a dormancy phase (17).

Arnica montana is difficult to cultivate, and extensive harvesting across Europe has led to a decline in wild populations. *Arnica montana* can be introduced through seeds, rosettes, or by clonal propagation. Compared with cultivation through seeds and rosettes, clonal propagation is more productive, with ramet formation and flowering occurring within the first year (18). However, through seed introduction, one recent cultivation trial of three wild accessions found that within the first year neither accession had produced a flower, but by the second year, the average flowers per plant grew to 12.5, with a dry yield of 22.6 g/m² (19). The dry flower production results given by this trial are similar to a 2004 study that found a dry flower production yield of 25-53 g/m² (20).

The harvesting of *A. montana* as a natural treatment for inflammation is not sustainable in its current form. Though protections have been implemented by governments across Europe, the population has been dramatically declining due to overharvesting and environmental change. Furthermore, research into different methods of cultivation have yet to increase yields significantly enough to protect wild populations. A collapse of *A. montana* populations from their native environments across Europe would represent a further loss of biodiversity. To alleviate the stress on *A. montana*, a new species of plant containing the anti-inflammatory properties (through the same biochemical mechanism) must be identified. For this reason, a relatively under-researched genus, *Eupatorium*, is a candidate for further study.

Eupatorium serotinum

The genus *Eupatorium* is known to include over 1200 species scattered across Africa, Asia, Europe, and the Americas (21). There are many documented uses of eupatorium species in Native North American folk medicine, many of which attribute the plants with anti-inflammatory properties. *Eupatorium serotinum*, also known as white boneset or late-flowering thoroughwort, has been used to *E. capillifolium* (dog fennel) has been long used as a treatment for insect bite in North America. In Argentinian folk medicine *E. laevigatum*, *E. arnottianum* and *E. subhastatum* have been used and further researched for their ability to relieve inflammation (22). Many species in the genus have been used to

treat ailments not related to inflammation as well. Both *E. purpureum* (gravel root) and *E. maculatum* (snakeweed) have been used to treat kidney ailments since at least the 19th century in North America. *Eupatorium purpureum* has also been used by the Meskwaki people of the Great Lakes region as an aphrodisiac (23).

Eupatorium serotinum is a rhizomatous perennial species in the Asteraceae family. It is native to the southern United States and Mexico. It is considered an invasive species to the U.S. Northeast, and many previous attempts at eradication there have been successful (24). Though multiple species of *Eupatorium* exist in the United States, *E. serotinum* is the most locally abundant in the Nacogdoches area. Like other members of the *Eupatorium* genus, *E. serotinum* is a rhizomatous perennial plant, which is relatively large, growing up to 2 meters in height. The plant produces large (5–14 cm × 2–3.8 cm) serrated leaves that run opposite along the stem. Flower buds form in late February, blooming around June, and remain visible until early winter (25).

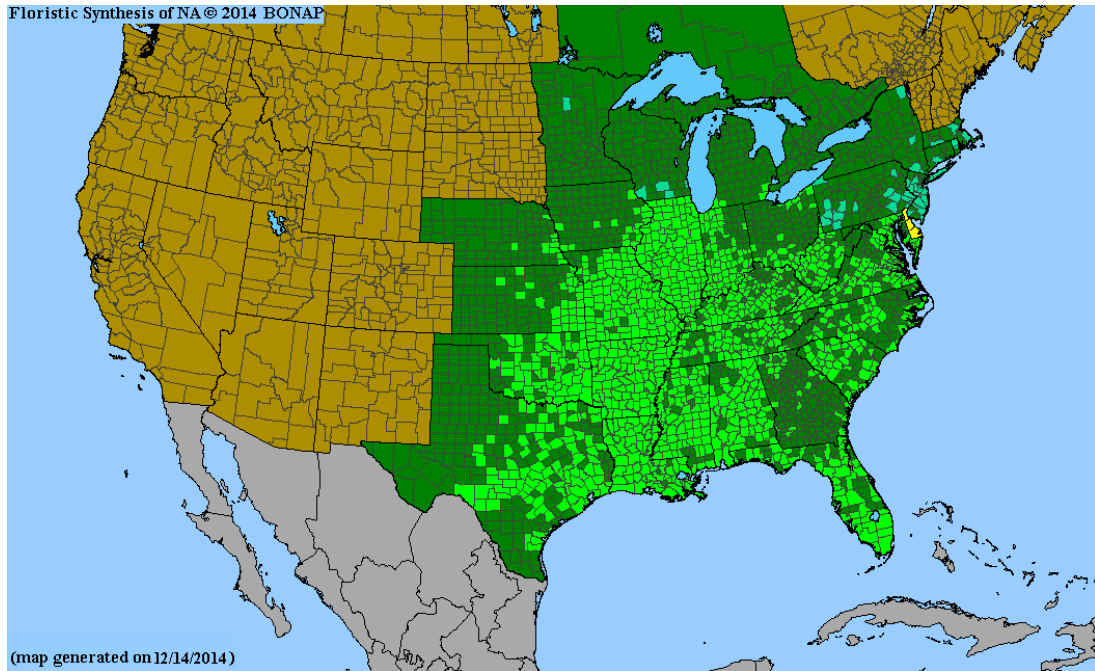


Figure 1. *Eupatorium serotinum* Distribution - Biota of North America Program (BONAP)

As it produces rhizomes, this species can be observed growing in dense groups in the wild. The seeds are relatively small (1.5mm in length), and are wind dispersed. For this reason it can be a difficult species to control, and infestations have occurred as far away as Australia (26). The combination of these factors - the dense growing clusters, tall stems, bright white bulbs, and unique leaf shape - allow for easy identification of *E. serotinum* in the wild.



Figure 2. *Eupatorium serotinum* - University of Southern Florida, Institute for Systematic Botany

Eupatorium serotinum is the ideal species to harvest for this study. The genus *Eupatorium* is already known, in folk medicine, to have anti-inflammatory activity. Should a similar anti-inflammatory compound in *E. serotinum* be identified as in *A. montana*, there would be immediate economic and ecological benefits to this substitution. Geographically, *A. montana* grows only in Europe, (though with a declining area of distribution) and has proven to be difficult to

cultivate. Meanwhile, *E. serotinum* has a distribution that ranges from Mexico to the north eastern United States, and grows so quickly that it is considered to be an invasive nuisance to areas it becomes introduced in. Harvesting of *E. serotinum* could thus be part of a responsible environmental management policy.

Project Overview

Folk medicine has been used to treat diseases related to inflammation for centuries. In many cases, the underlying mechanism of action or scientific validation of the anti-inflammatory properties continue to go unstudied. In the case of *Eupatorium serotinum*, we sought to determine whether we can identify anti-inflammatory properties in crude extractions from the plant material.

First, we searched areas of East Texas that can support populations of *E. serotinum*. Using classic plant identification methods such as the determination of leaf and stem morphology as discussed earlier, we identified a group of wild-growing *Eupatorium serotinum*. The whole plant was harvested including the roots, and taken back to Stephen F. Austin State University to be cleaned and processed. A plant press was used to press and dry one whole plant for the creation of a voucher specimen and further identification in a qualified Herbarium.

An ethanol extraction was performed on the remaining plant material and that extract was further concentrated with a rotovac. From there, toxicity was determined using cell death and MTT assays. High Performance Liquid Chromatography (HPLC) was performed on the extracts to identify sesquiterpene

lactones. Finally, an inflammation assay was performed to determine the anti-inflammatory properties of the extract.

Inflammation Pathway

Inflammation is a complex immune response characterized by swelling, pain, and increased temperature of the diseased area. This process is the result of a coordination of tissue and cells and is mediated by a variety of chemical messengers (27). Under normal circumstances, inflammation aids in wound healing and tissue repair, however, several diseases can arise due to chronic and improper inflammation in many areas of the body. Rheumatoid Arthritis is caused by chronic inflammation in the joints, and can cause symptoms such as pain, swelling, and redness (28). Asthma is caused by chronic lung inflammation in which the airways become narrow. Symptoms include coughing and shortness of breath (29). Chronic inflammation of the digestive tract can lead to Inflammatory bowel disease (IBD), which can cause abdominal pain, nausea, and weight loss (30).

At the cellular level, inflammation begins as a response to either infection or tissue damage. In the case of infection, host immune cells can recognize foreign molecules called “pathogen-associated molecular patterns” or PAMPs through the toll-like receptors on their cell membranes or within their cytoplasm. This triggers a cascade of signaling events which leads to the activation of the cell's inflammation response, and the release of inflammatory cytokines (31). In

the case of tissue damage, a variety of signals are released called “damage-associated molecular patterns” or DAMPs, which similarly activate the inflammatory response pathway in healthy immune cells (32). When the immune cells recognize the PAMPs or DAMPs, they release TNF- α which further stimulates the immune response in other cells (33).

Non-immune cells such as endothelial cells can also recognize TNF- α and respond accordingly. When these vessel lining cells detect TNF- α through binding to its TNFR receptors, a signal cascade is activated within the cells which leads to the activation of NF- κ B. This leads to the upregulation and release of various signaling molecules which recruit immune cells to the site (34).

NF- κ B is an important transcriptional regulatory protein for the modulation of immune regulatory genes. Composed of two subunits, NF- κ B exists in its deactivated form in the cytosol, and is accompanied by the inhibitory molecule I- κ B. In the cytoplasm, NF- κ B usually exists as homodimers or heterodimers of a family of related proteins. Among these proteins are RelA (also called p65), c-Rel, RelB, NF- κ B1 (p50/105), and NF- κ B2 (p52/p100) (35). Following the phosphorylation, ubiquitination, and proteolysis of I- κ B, NF- κ B translocates into the nucleus where it induces transcription of various immune related genes.

Gene regulation, similarly to other transcription factors, occurs through the physical binding of the NF- κ B complex to specific promoter regions downstream of the target genes. Multiple pathways exist for the activation of NF- κ B, among

these are cell stimulation by lipopolysaccharide (LPS), or stimulation by TNF- α . Among the target genes upregulated by NF- κ B, are the Immunoreceptors (Immunoglobulin, IL2, Tissue Factor), cell adhesion molecules (ELAM-1, VCAM-1, ICAM-1), Cytokines (TNF- α , IL-2, IL-6, IL-8, IL-12), Chemokines (MIP-1alpha, and MIP-2), as well as various other proteins and transcription factors (36).

For many decades, it was unclear what mechanism was employed by sesquiterpene lactones to inhibit immune response. In 1997, it was discovered that helenalin, the sesquiterpene lactone from *Arnica montana*, inhibits the activation of NF- κ B. This inhibition is not due to a modification of the active NF- κ B heterodimers, rather it is due to the modification of the inactivated NF- κ B/I- κ B complex. The modification prevents the release of I- κ B (37).

The effects of this modification can be visualized by an electrophoresis mobility shift assay (EMSA.) EMSA is a technique that detects protein complexes with nucleic acids. Much like a traditional Gel electrophoresis for DNA separation, EMSA uses either an agarose or polyacrylamide gel to run a solution containing the protein of interest with the dsDNA target. If the solution forms a protein-nucleic acid complex, the bands will appear to move more slowly compared to the dsDNA control (38).

Anti-Inflammatory Drugs and Sesquiterpene Lactones

Inflammation can be expressed chronically or as a temporary reaction to foreign invaders. Symptoms of inflammation include swelling, pain, soreness, and difficulty of motion. Modern anti-inflammatory compounds include corticosteroids, which are hormones with very potent anti-inflammatory effects. However, they are only recommended to be used in low-doses over a short period of time due to adverse reactions when taken for longer periods (39). NSAIDS work by inhibiting the activity of cyclooxygenase enzymes COX-1 and COX-2, which prevents the formation of prostaglandins, thus reducing inflammation and pain (40). However, gastric and cardiovascular damage can result from the continued use of NSAIDS due to the inhibition of prostaglandin production (41).

Prior to the development of these modern anti-inflammatory compounds, historical methods of inflammation management were limited to herbal and folk remedies. Recent studies of many plants used in ancient folk medicine have led to the discovery of anti-inflammatory compounds with novel mechanisms of action. Most notably, *Arnica montana*, has been popular among researchers looking for substitutes to the current anti-inflammatory regiment. *Arnica montana* also known as mountain tobacco, mountain arnica, or wolf's bane has been used in traditional medicine in Europe for thousands of years. More recently, the anti-inflammatory activity of *A. montana* has been linked to its production of Helenalin

belonging to a class of biologically active molecules called sesquiterpene lactones. However, the population of *A. montana* has been on a steep decline due to over-harvesting for medicinal use as well as environmental degradation. It is clear that the identification of a new medicinal plant with similar anti-inflammatory compounds would be beneficial, both to the treatment of inflammation, as well as to the preservation of *A. montana*.

One class of bioactive molecules found in thousands of plant species is sesquiterpenoids Lactones (SLs). The SL Helenalin has been identified as the causative agent for the anti-inflammatory activity of *A. montana*. These compounds are found across the plant kingdom, but are most prevalent in *Asteraceae* (42). SLs are composed of carbocyclic skeletons, and are differentiated into four classes: germacranolides (with a ten-member ring), eudesmanolides (with two 6-member rings), guaianolides, and pseudo guaianolides (43). Previous studies have determined that structurally distinct SLs reduce inflammation in *in vivo* models (44). Further studies support the mechanism of action for SLs derived from Arnica as well from other Mexican Indian medicinal plants due to the inhibition of transcription factor NF- κ B (45).

High Performance Liquid Chromatography

High Performance Liquid Chromatography (HPLC) is a widely used analytical chemistry technique. HPLC is used to separate, identify and quantify the chemical components of a mixture. This technique is often used for quality

control and drug discovery (46). HPLC was first described in the 1960's, and works by resuspending a mixture in a "mobile phase" then passing the suspension through a "stationary phase" or tightly packed column. This occurs under a high pressure, sometimes reaching 60 MPa. As the compounds in the mobile phase pass through the stationary phase column, they separate based on chemical properties. As the compounds exit the column at different retention times (RT), they are measured by a variety of detection methods including UV absorption or fluorescence (47). Identification and quantification of a specific compound in a mixture can be achieved by running a series of the pure compound through the HPLC at different concentrations. As a pure compound, the chromatogram should show a single peak, and the area of the peak will be proportional to the concentration of compound in the sample. This allows for the creation of a standard curve in order to estimate the concentration of the compound in the sample mixture.

Depending on the mixture and type of compound being identified, the composition of the mobile phase and stationary phase can be adjusted to allow for better resolution. The stationary phase is commonly composed of solid supports such as a non-polar silica gel, that interact with chemical groups in the resuspended compounds. The difference in interaction between different chemical compounds causes a difference in retention time (48). The mobile phase usually consists of a mixture of several solvents including water, methanol,

acetonitrile, or tetrahydrofuran. The composition of the mobile phase can be changed throughout the run to create a gradient. Gradient elution can be used to improve the separation of compounds from complex mixtures (49).

Human Cell Culturing

For the discovery of the pharmaceutical properties of novel compounds or extracts, it is customary to begin with in vitro models involving the culturing and treatment of human cells. The culturing of human cells is a much more delicate and resource intensive activity than bacterial cell culturing due to many factors. One of the main challenges is to ensure a sterile environment for the cells to grow. Cell culture media that human cells use is also an acceptable media for bacteria to propagate in. Since bacteria have a faster doubling time, and the human cell line is being grown outside the body without a complement of natural immune cells, it can be quickly outcompeted by bacterial contamination (50).

Another thing to consider is the method of growth. Some cell types can be grown in suspension, while others grow better adherently. Adherent cells require a cell culture flask or plate that is coated with a hydrophilic substrate such as collagen, fibronectin, or poly-L-lysine to enhance cell adhesion (51). A benefit of growing cells adherently is that morphology and cell density can be easily estimated by using a microscope, while cells grown in suspension must be counted either by an automated cell counter or with a hemocytometer. The latter

being a more labor and time-consuming method, especially when cell density should be recorded at least once a day.

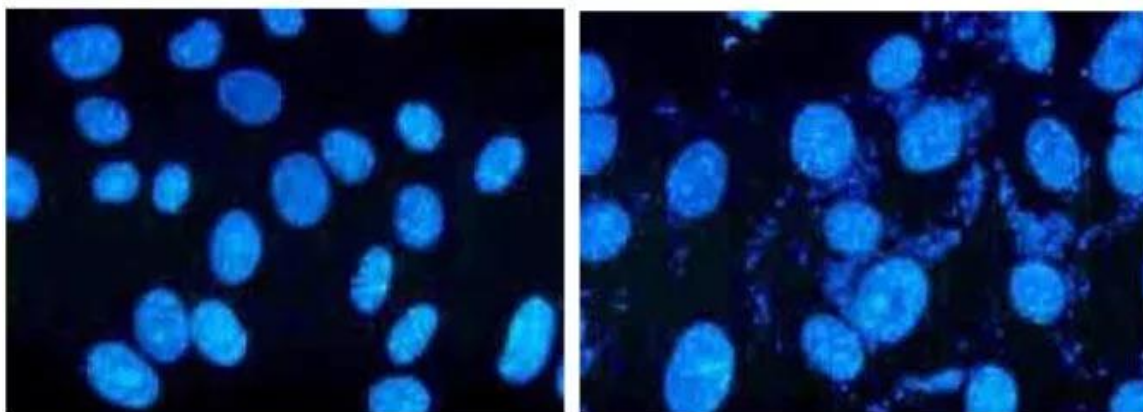
Finally, it is important to carefully control cell propagation and move the cells into a new environment to prevent overcrowding. The movement of cells from one adherent flask to another at a lower density is called “passing.” Gene transcription can change dramatically depending on whether the cells are in the log phase of growth or in the stationary phase. Cells that are overcrowded revert to the stationary phase. Because of this, cells are intentionally plated at a relatively low “seeding density” (the number of cells incubated in a flask per square centimeter of area) and allowed to grow until around 80%-90% confluence. Confluence is a measurement of the crowing of cells, and represents the percent of area occupied by cells when viewed under a microscope. This confluence number is recorded each day, so that the doubling time can be monitored, and the cells can be passed into a new flask before overcrowding (50).

As cells continue to divide and are continuously passed into new flasks, they begin to suffer from morphological and metabolic defects due to the number of divisions. This type of aging is called senescence, and eventually leads to a cell line that grows too slowly to be practical for continued culturing. Furthermore, senescence can also lead to changes in protein production and gene expression, making a cell line unsuitable for further testing, as the results would not

necessarily reflect normal cell behavior. For this reason, cell cultures are assigned “passage numbers” which increase each time a cell line is passed into a new flask. Most cell types can have a passage number over 20 before displaying the effects of senescence. Reliable data should be gathered from cells of the lowest practical passage number (50).

Mycoplasma contamination testing should also be done on cells being cultured for use in an RNA differential expression analysis. Mycoplasma contamination is a common challenge in cell culture maintenance, affecting approximately 35% of all frozen cell stocks. Mycoplasma are a small genus of bacteria that lack a cell wall or peptidoglycan, making them naturally resistant to antibiotics that target cell wall synthesis. Contamination can lead to changes in cell morphology, gene expression, and growth rate (52).

Several methods for detecting mycoplasma contamination exist such as PCR assays or ELISAs. One of the most cost-effective methods to detect mycoplasma is by the use of Hoechst staining. Hoechst dyes are bis-benzimides that bind to DNA and emit a blue light upon excitation with UV light (52). By viewing the microscopic images of cells stained with Hoescht dye, the presence of mycoplasma contamination within the cell can be detected (53). Mycoplasma appear as streaks or stains of blue fluorescent light outside of the cell nucleus, while uninfected cells have a clearly defined nucleus with no blue light appearing outside of it (Figure 3).



Photomicrographs (1000X) of VERO cells stained with Hoechst 33258 dye. DNA-containing nuclei and mycoplasma stain brightly under ultraviolet light allowing the clean culture (left) to be easily distinguished from the infected culture (right). (Photomicrographs courtesy of Bionique Testing Laboratories.)

Figure 3. Mycoplasma Contamination Testing with Hoechst Dye

Uninfected cells (left) can be seen with a clear circular nucleus dyed blue. There is no blue light outside of the nucleus. On the right are cells infected with mycoplasma. The DNA in the mycoplasma creates streaks or stains of blue light outside of the host cell nucleus. Hoechst staining is an effective tool to detect mycoplasma contamination.

HEK293 Cells

HEK293 cells (human embryonic kidney cells) were originally isolated from the kidney of a healthy fetus in 1973. They are highly stable and show consistent morphological and metabolic characteristics over a long period of time (54). These cells display a robust stability, versatility, and have a relatively fast

growth rate of around 16-24 hours depending on growth conditions. They can be cultured either in suspension or adherently with cell culture treated flasks. This cell line also displays high transfection efficiency, making them ideal cell lines for the study of cellular pathways and recombinant protein expression (55).

Due to their ease of use, they have been well studied since their isolation. HEK293 cells are still widely used in biological research especially in the development of cell-based assays and vaccines. They are also used to determine drug-target interaction and to study the function of disease-related genes and proteins (56). Although not an immune cell, HEK293 cells express low levels of TNFR, a receptor for TNF- α . For this reason, they are ideally suited for immunosuppressant studies of novel compounds.

Cytotoxicity Testing

Before immunological or other pharmaceutical properties of a novel compound or extract can be tested on a human cell line, it is first necessary to determine the *in vitro* toxicology of the sample. There are many ways of performing a toxicology analysis, but all involve the use of cultured cells treated with increasing doses of the sample of interest. *In vitro* testing of toxicology can also be expanded to determine the mechanisms of toxicity (57).

One way of determining the toxicity of a compound is with an MTT assay. This assay involves the treatment of a cell culture in a 96 well plate to the compound at increasing concentrations. The treated cells are allowed to incubate

for approximately 24 hours. They are then treated with MTT (3 - (4, 5 - dimethylthiazol - 2 - yl) - 2 , 5 - diphenyltetrazolium bromide) which is a yellow colored tetrazolium dye. Metabolically active cells will be able to reduce this dye to formazan which has a purple color. The insoluble formazan crystals can be dissolved in DMSO or an acidified isopropanol solution, and the absorbance of the wells is read at 550 nm. The absorbance at 550 nm is directly proportional to the metabolic activity of the cells in each well (58).

Toxicity can also be tested by a simple live cell count following the same 24-hour treatment of the sample of interest. In this experiment, cells are grown in a larger 6-well plate and treated with the sample of interest. Following the incubation period, the cells are passed from the wells and counted using a hemocytometer and trypan blue. Trypan blue can differentially stain dead cells blue while leaving live cells transparent in color. This is caused by the negative charge of the dye preventing the molecule from entering the plasma membrane of live cells. Dead or dying cells will have perforations in their membranes, allowing trypan blue to migrate in and bind to intracellular proteins and nucleic acids (59). The number of live cells following treatment at different concentrations can be used to determine the toxicity of the sample.

Differential Expression Analysis

Differential gene expression analysis of transcriptomic analysis is a powerful method to determine the effect of a sample of interest on the gene

expression of a cell line or organism. In this project, I used this to determine the immuno-suppressant properties of our crude extractions from *Eupatorium serotinum* on HEK293 cells. Briefly, HEK293 cells will be pretreated with our compound of interest before being exposed to TNF- α . TNF- α is a chemical messenger which activates the NF-kappaB related gene expression changes. In a differential expression study, the total mRNA of the cells in a dish are extracted and sent for sequencing to determine global gene expression following the treatment of a certain compound or series of compounds.

Messenger RNA or mRNA is the molecular mediator of genetic information from the nucleus (where it is stored as double stranded DNA), to the ribosomes where the mRNA is translated into protein products. The entirety of the mRNA in a cell at a given time is called the transcriptome. This study is often called a transcriptomic analysis. In the case of this project, we would expect to find that NF-kappa B related genes are upregulated in response to TNF- α stimulation. However, if our extract is immunosuppressant, and that suppression is similarly caused by the prevention of NF-kappaB activation, then we expect that the cells pretreated with our extract to not show the same upregulation in NF-kappaB related genes in response to TNF- α stimulation. Furthermore, differential expression can also help to identify other effects the extract may have on human cells in-vitro, as the entire transcriptome will be measured (60).

The first step in a differential expression study is the isolation of RNA from the treated samples. RNA can be isolated by a standard TRIzol extraction procedure. TRIzol is a common reagent used in RNA isolation, and is a mixture of guanidinium thiocyanate, phenol, and chloroform (61). This solution allows for the denaturation of proteins (including nucleases), the perforation of the cellular membranes, and the release of RNA. The total RNA can be precipitated out using ethanol, then stored in a buffer containing EDTA to prevent RNA degradation (62).

Total RNA sequencing of the mRNA from our samples involves a high-throughput sequencing method called Next-generation sequencing (NGS). The first generation of DNA sequencing involved the use of Sanger sequencing technology developed in the 1970's. Sanger sequencing involves the fluorescent or radioactive labeling followed by gel electrophoresis to separate strands by size. This method was limited by its high cost, high manpower requirements, and low-throughput (63).

NGS was first used in 2005, and has allowed for much more high-throughput sequencing of DNA and RNA. This is achieved by fragmenting the transcripts and then ligating them to adapters. These adapters allow the transcripts to attach to a specific point on the sequencing surface. Amplification occurs which incorporates nucleotides designed to give off a fluorescent signal during incorporation by DNA polymerase. Each nucleotide gives off a unique

fluorescent signal, and high-powered cameras detect and record the incorporation of each strand. This allows for many strands of DNA to be sequenced in parallel (64).

Finally, the sequencing data is analyzed using a series of bioinformatic programs to determine the differential expression of genes between samples. The data containing all of the mRNA reads is sent in a large FASTQ file. A FASTQ file is a text-based file format that includes the nucleotide sequence of each read from a sequencing run along with the quality score which measures how reliable the call was. Reads with low reliability should be discarded in favor of reads with higher reliability. This is done by assigning a quality score threshold and filtering out the reads that do not meet the standard for reliability. This can be done using a program called FastQC (65).

Next, the reads must be aligned to the reference genome. In this case, our reference genome is the human genome, which is well annotated for coding sites. To do this, a read-alignment program such as HISAT2 must be used. This program will generate a BAM file that represents the mapping of the reads to the reference genome. Afterwards, a count matrix for each gene must be generated to quantify the expression levels. This can be achieved with a program called htseq-count (66).

The count matrix for each BAM file can now be analyzed for differential expression relative to our control sample. To do this, a program called DESeq2

can be used which identifies any differentially expressed gene between the BAM file of the treated sample and the BAM file of the control. The output of this program is a list of all differentially expressed genes along with the statistical significance and their log-fold change. This data can be used to generate a volcano plot showing the most significantly upregulated and downregulated genes between a sample and the control (67).

MATERIALS AND METHODS

Field Collection of *Eupatorium Serotinum*

Multiple sites across East Texas were surveyed for *Eupatorium serotinum*. Survey sites were selected based on a criteria which represents the preferred environment of *E. serotinum*. These sites were located throughout Nacogdoches, Denton, Brazos, and Wood counties. Sites included land clearings along public walking trails, public parks, empty lots along highways, and the SFA research forest. Specifically, we searched environments that had:

- Wide clearings of land
- Free from trees or branches which may obstruct the sunlight
- Undisturbed by human interaction (e.g. no mowing or clearing)
- Within the distribution range of *E serotinum* given by the map in Figure 1.

A group of *E. serotinum* was spotted and preliminary identification was done based on the known morphology of the plant. This includes alternate serrated leaf patterns, a stem height of around 2 meters, white late-blooming florets, and branching stems. The specimens were collected in Wood County at Holly Lake Ranch, Texas, 75765, south-west of the intersection between Cimarron Trail and Laurel Lane (32.715566, -95.1717340). The local flora was photographed and nearby species were also identified based on morphology.

The specimens were dug from the ground using a shovel and spade, and were transported in bags back to the archeology laboratory at Stephen F. Austin State University.

Preparation of Herbarium Voucher Specimen

Plant specimens were removed from their packaging and prepared in the archeology laboratory at Stephen F. Austin State University. Prior to processing, the specimens were photographed and measured. The roots were cleaned with water to remove any dirt. One specimen was set aside for ethanol extraction, while the other four samples were processed to make herbarium voucher specimens.

Voucher specimens were prepared by fitting the entire plant into an area of no more than 29.2 by 41.9 cm (11.5 by 16.5 inches). Due to the size of the plant, it was necessary to break and bend the stems multiple times in order to get the entire sample to fit within the area. Stems and leaves were cut and removed so that no plant material was overlapping or obstructed. Leaves were arranged so that they were fully visible, without folding, and the venation could be clearly seen. A total of four samples were prepared.

The voucher specimens were dried and pressed on a plant press. The plant press was constructed with 1/2" x 2" wooden boards. The press itself was 30.48 x 45.72 cm (12 by 18 inches) and was composed of five wooden boards running vertically against two horizontal boards. The voucher samples were

layered between alternating sheets of newspaper and cardboard to allow for proper aeration. The newspaper/cardboard/plant material was put between the two sides of the plant press, and 5 kg of weight was added to the top of the press. The plant press was placed in a fume hood with a space heater so that the ambient temperature was 35°C (95°F). The plants were dried for approximately two weeks before transporting them to the S.M. Tracy Herbarium at Texas A&M University. At the herbarium, the voucher specimens were mounted onto herbarium paper and identified as *Eupatorium serotinum*.

Crude Ethanol Extraction

Before preparation of the specimen for ethanol extraction, the plant was washed gently but thoroughly with running water to remove any dirt, insects, or other debris. The specimen was cut and separated into its roots, stem, leaves, and florets. The plant material was weighed before being put into a 950 mL mason jar. The jar was filled with 95% ethanol, and set in a dark location at room temperature for approximately two weeks. Following extraction, the solution was filtered through a woven metal fiber filter to remove plant debris and collected in a sealed plastic container. This crude extraction was further concentrated by evaporating the excess ethanol in a rotovac for approximately 30 minutes at 37°C and 100 mbar. These concentrated ethanol extracts were stored at 4°C until further use.

HEK-293 Cell Culturing

HEK293 Cells are a product of Gibco and were purchased from ThermoFisher Scientific. They are adapted to grow in serum-free 293 media supplemented with glutamine and antibiotic-antimycotic. The media used was serum-free CD 293 media purchased from ThermoFisher. Media was prepared by adding 2.5 mL of 100x Antibiotic-Antimycotic containing 10,000 units/mL of Penicillin and 10,000 ug/mL of Streptomycin to 1 liter of CD 293 media. 20 mL of 200mM GlutaMAX was also added. Finally, 10% FBS was also added to the culture media before filter sterilizing with a 0.2 micrometer filter. Culture media was stored at 4°C when not in use.

HEK293 cells arrived in a vial of 7.5×10^6 cells stored at -80°C. Following the manufacturer's protocol, cells were thawed quickly in a 37°C water bath for approximately 1 minute. The contents of the vial were transferred into a 125mL shaker-flask containing 30 mL of freshly prepared culture media warmed to 37°C. This was labeled as P0. The cells were grown on an orbital shaker at 120 rpm with a loosened cap to allow for gas exchange. The shaker was placed in an incubator set to 37°C and supplemented with 8% CO₂. The cells were grown until they reached a cell density of between 2×10^6 - 3×10^6 viable cells per mL. Cell count and viability was monitored daily by the cell counter. Following the growth of P0 to 2×10^6 to 3×10^6 viable cells per mL, the cells were subcultured onto plates, wells, or cryogenically stored.

Further subculturing proceeded according to the protocol provided by ThermoFisher. Briefly, cells were plated in flasks at a seeding density of 5×10^4 viable cells per cm^2 in 2.5 mL culture media per 10 cm^2 . Cell cultures were maintained in an incubator set to 37°C and supplemented with 8% CO_2 . Each day, the flasks were carefully removed from the incubator and observed under a microscope to mark the confluence. Once cells reached 60-80% confluence they were passaged into a new flask. This was achieved by aspirating the media from the flask then adding 5mL / 75 cm^2 TrypLE™ prewarmed to 37°C to the flask. The flask was incubated at 37°C for 5 minutes, then the cells were detached by forcefully rapping the flask by hand. 5 mL of culture media was added to the flask, and the flask was tilted in all directions to ensure resuspension of cells into the liquid. The liquid was poured into a 50 mL conical tube and centrifuged at 100g for 5 minutes. The supernatant was aspirated and the pellet was resuspended in 10 mL of culture media. Viable cells were counted as described earlier, and a new flask was prepared at a seeding density of 5×10^4 viable cells / cm^2 .

Toxicity Testing - Cell Death Assay

Cells were passed into a six-well plate at a seeding density of 3.0×10^4 cells per cm^2 . Two milliliters of cell culture media was added and the cells were incubated at 37°C , 8% CO_2 in a humidified atmosphere. Each day, confluence was recorded by observing the cells under a light microscope. Once the cells

reached a confluence of 75%, they were treated with different concentrations of our extract or sample of interest. Some culture media was removed before treatment to keep the total volume of the media in each well at 2 mL. The cells were further incubated for 24 hours before counting.

Cells were counted by using the trypan blue differential staining technique. Briefly, following 24 hours of treatment, the media was collected into 15 mL conical tubes. The media wasn't discarded in case live cells lost their adherence and were resuspended in the media. To detach cells, 0.5 mL of TrypLE was added to each well, and the plates were incubated for 3 minutes at 37°C. The contents of the wells were mixed well by pipetting and transferred into the same 15 mL conical tube containing the old media. Cells were centrifuged for 5 minutes at 200 x g. The supernatant was discarded and the pellet was resuspended in 2 mL of culture media.

Following resuspension, 100 microliters of the resuspended cell culture were added to a microcentrifuge tube along with 10 microliters of trypan blue. The tube was mixed well by flicking or inverting (to avoid damaging the live cells). Following incubation at room temperature for 3 minutes, 10 microliters of the cell culture mixture was transferred to a hemocytometer. Four 0.1mm x 0.1mm squares were counted to get an average live and dead cell count for the sample. This process was repeated for each well.

Toxicity Testing - Cell Viability Assay

Cells were passed into a 96-well plate at a seeding density of 5.0×10^4 cells per well. 0.2 mL of cell culture media was added to each well and the cells were incubated at 37 °C, 8% CO₂ in a humidified atmosphere. Each day, confluence was recorded by observing the cells under a light microscope. Once the cells reached a confluence of 75%, they were treated with different concentrations of our extract or sample of interest. The treatment groups were done in triplicate to account for pipetting errors. The cells were further incubated for 24 hours before determining viability.

Cell viability was determined by using the CellTiter 96® AQueous One Solution Cell Proliferation Assay. Briefly, all 200 µL of media was removed and 100 µL of fresh culture media along with 10 µL of AQueous One Solution reagent was added to each well. The 96-well plates were further incubated for 4 hours at 37 °C. After 4 hours, the absorbance of all wells at 490 nm was measured using a 96-well plate reader.

Mycoplasma Contamination Testing

Cells were passed into a 6 well plate with a glass coverslip secured to the bottom of the well. The seeding density was 3.0×10^4 cells per well. 2 mL of cell culture media was added to each well and the cells were incubated at 37 °C, 8% CO₂ in a humidified atmosphere. Each day, confluence was recorded by observing the cells under a light microscope. Once the cells reached a

confluence of 80-90%, the media was aspirated and the slides were fully covered with Hoechst staining solution at a concentration of 5 µg/mL. The stain was incubated for 10 minutes before washing the slides gently with PBS. The cover slip was fitted to a glass slide then viewed under a UV microscope. Pictures were taken through the lens and included in the results.

Inflammation Assay

Cells were passed into a 10 cm diameter tissue culture plate at a seeding density of 3.0×10^4 cells per well. Twelve milliliters of cell culture media were added to each well and the cells were incubated at 37°C, 8% CO₂ in a humidified atmosphere. Each day, confluence was recorded by observing the cells under a light microscope. Cells were treated with extract once they reached a confluence of 75%. Plates 1 and 2 were pretreated with 0.2 % (v/v) of PBS extract for 1 hour. Plates 3 and 4 were pretreated with .05% (v/v) of ethanol extract for 1 hour. Plates 5 and 6 were pretreated with 10µmof helenalin. Following the hour of pretreatment plates 2, 4, 6, and 7 were treated with 50ng/mL of TNF-α and incubated for 1 hour. Plate 8 was a control and received no treatment. Following the 1 hour treatment with TNF-α, RNA extraction was performed.

RNA Extraction

RNA was extracted using TRIzol according to the manufacturer's protocol. Briefly, cell culture media was removed from the plates and 500µl of TRIzol was added directly to the dish. The lysate was homogenized by pipetting up and

down. The plates were incubated for 5 minutes at room temperature. The lysate was transferred to a microcentrifuge tube and 100µl of chloroform was added. The tube was vortexed and incubated at room temperature for 3 minutes. The tubes were centrifuged for 15 minutes at 12,000 x g at 4°C. The aqueous phase containing the RNA was carefully transferred to a new tube by pipetting and the rest was discarded, and 100µl of isopropanol was added. The solution was mixed by pipetting. The tubes were incubated for 10 minutes then centrifuged for 10 minutes at 12,000 x g at 4°C. The supernatant was discarded and the RNA was washed by resuspending it in 500 µl of 75% ethanol. The tube was centrifuge for 5 minutes at 7,500 x g at 4°C. The ethanol was removed by pipetting and the sample was left to dry for 5 minutes. The RAN was resuspended in 100µl of pH 8.0 TE buffer and stored at -80°C until shipment.

Transcriptomic Analysis

RNA was sent to the Novogene facility in Sacramento, California for sequencing. Novogene performed QC assays to determine the purity and concentration of RNA and performed electrophoresis to estimate the size of the fragments. RT-PCR was performed and the appropriate primers with adapters for downstream next-generation sequencing (NGS) were added. NGS was then performed by Novogene and the data was sent back in FastQ files.

Each FastQ file was processed for read quality using FastQC. The reads were aligned to the human reference genome using HISAT2, which generated a

BAM file containing the reads mapped to the reference genome. The BAM files were analyzed with htSeq-count to generate a count matrix for each gene. Finally, DESeq2 was used on the outputs to determine differential expression.

HPLC

The samples were prepared by further filtering the extractions through a .2µm filter to prevent any large particulates from clogging the solid phase during the procedure. Helenalin was ordered and the lyophilized powder was resuspended in ultrapure water. Filtered extracts were further diluted with ultrapure water before testing. The procedure was performed using Jasco instrumentation. The samples were loaded with a Jasco AS-4050 autosampler, and the pump was a Jasco PU-4180. Ten microliters were injected per sample. The photodiode array (PDA) was a Jasco MD-4010. The solid phase was a reverse phase Phenomex Kinetex column (5-micron, 100 angstrom, C-18). with a silica hydrophobic column for the solid phase. The liquid phase was composed of solution A (10% methanol solution) and solution B (pure methanol). The sample was run for a total of 70 minutes. To further resolve the peaks, the liquid phase was run as a methanol gradient. From 0 to 4 minutes the mobile phase was 17% solution A and 83% solution B. From 4 to 55 minutes the mobile phase was 100% solution A. From 55 to 65 minutes the mobile phase was 17% solution A and 83% solution B.

RESULTS AND DISCUSSION

Plant Collection and Herbarium Voucher

Eupatorium serotinum plants were identified by morphology in Wood County at Holly Lake Ranch, Texas, 75765, south-west of the intersection between Cimarron Trail and Laurel Lane (32.715566, -95.1717340). There were approximately 15 plants growing within a 5-meter radius of each other. A picture of the plant before harvesting is given in Figure 8. The samples were transported back to SFA where one was cleaned, processed by removing excess branches and leaves, and dried under a plant press to produce a voucher specimen. This specimen was transported to the Texas A&M, S. M. Tracy Herbarium located at 3380 University Dr E #131, College Station, TX 77845. Here, the sample was identified by the herbarium as *Eupatorium serotinum*, photographed, and moved into long-term storage (Figure 5).



Figure 4. *Eupatorium serotinum* harvested from Holly Lake Ranch



Figure 5. *Eupatorium serotinum* herbarium voucher specimen



Figure 6. *E. serotinum* ethanol extraction jars

Eight of the samples taken from Holly Lake Ranch were used for extraction. The samples were cleaned and then processed by separating their flowers, leaves, stems, and roots into jars and measuring the mass. The mass of each component is as follows: 190 grams of plant stem, 84 grams of leaves, 124 grams of flower, and 96 grams from roots. The jars were filled with ethanol and left for two weeks (Figure 6).

The jars contain different plant components that were cleaned in water before separation. Ethanol was added to the jars and they were kept sealed at room temperature for two weeks. The solution was filtered through a coffee filter to remove the larger debris, and the final volume for each sample was as follows: Roots (730 mL), Flowers (580 mL), Leaves (700 mL), and Stems (590 mL). A combined extraction was prepared by a proportional amount of each extract to a jar (146 mL of root extract, 116 mL of flower extract, 140 mL of leaf extract, and 118 mL of stem extract for a total volume of 520 mL). The samples were then treated on a rotovac for 30 minutes to remove some of the ethanol. Half of the combined ethanol extract was treated again on the rotovac to completely remove the ethanol and the thick extracted material was resuspended in 100 mL of PBS.

HEK293 Growth and Mycoplasma Contamination

HEK293 cells were successfully cultured and expanded from the initial P0 tube containing 7.5×10^6 cells. All experiments took place between passage 1 and 5, and approximately 100 million cells were harvested and saved for future use. These were stored at -80°C and labeled with the date, passage number, initials, cell type, and number of cells. The doubling time of HEK293 cells in our culture media was approximately 12 hours.

Following the inflammation assay, HEK293 cells were used to seed a 6-well plate containing a glass cover-slip. The cells easily adhered to the glass cover slip and once the concentration reached 80% confluence, they were tested

for Mycoplasma contamination. The nuclei were observed under the microscope and no evidence of fibrils or clouds of non-host DNA were detected. The only irregularity seen under the microscope were thick blue streaks which was due to the smearing of some nuclei during the slide preparation process (Figure 7). This indicates that mycoplasma contamination was not present in our cell line by the time of the final experiment.

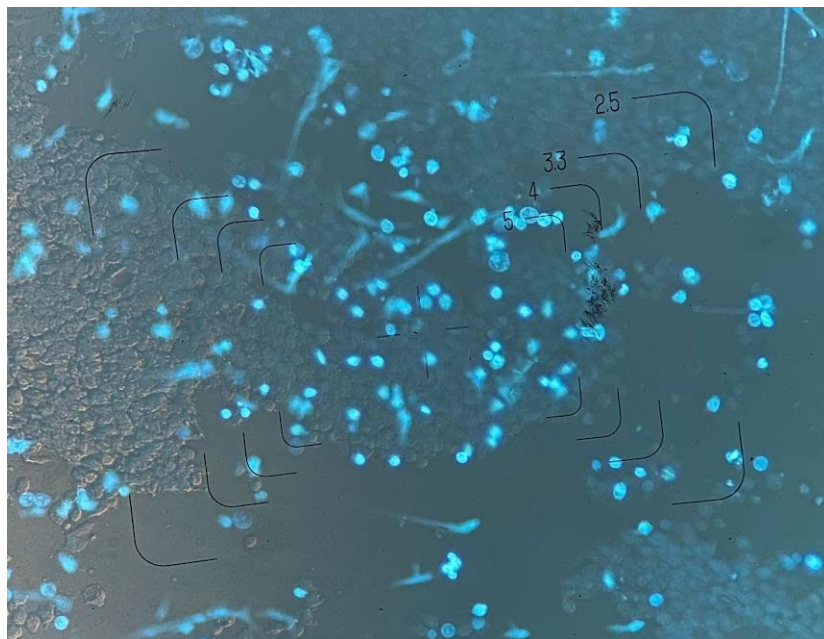


Figure 7. Mycoplasma contamination testing of HEK293 Cells

Cytotoxicity of Extractions

For the cell death assays (Figures 8 and 9), the cytotoxicity of the combined ethanol extract and the combined PBS extract was tested. Relative live

cells was calculated by dividing the number of live cells in the sample by the number of live cells from the untreated control group. A trendline was fitted to the data to calculate the LD50. The combined ethanol extract had an LD50 of 4.60 μl / mL, while the combined PBS extract had an LD50 of 18.5 μl / mL.

The cell viability assays were done in triplicate on a 96 well plate. The cytotoxicity of all extracts was determined. Relative cell viability was calculated by dividing the 570 nm absorbance of the sample by that of the untreated control. The data was fitted with a trendline to calculate the LD50. The combined ethanol extract (Figure 10) had an LD50 of 0.62 μl / mL, while the combined PBS extract (Figure 11) had an LD50 of 3.79 μl / mL. The LD50 for the leaf extract was 3.09 μl / mL (Figure 12), the stem extract was 34.61 μl / mL (Figure 13), the flower extract was 0.27 μl / mL, and the root extract was 58.0 μl / mL (Figure 14).

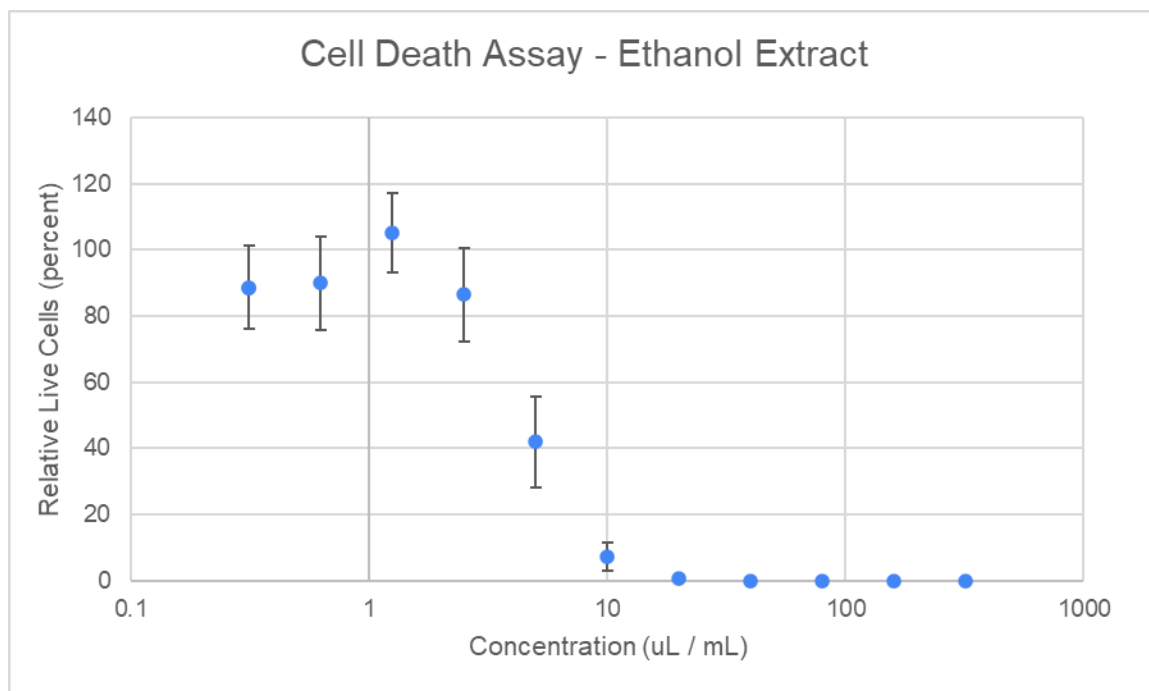


Figure 8. Cell Death Assay - Ethanol Extract

A cell death curve of HEK293 cells treated with the combined ethanol extract. A trendline is given by the equation $y = -57.2\ln(x) + 137.35$. The LD50 value is 4.60 $\mu\text{L} / \text{mL}$. Relative live cells was calculated by dividing the number of live cells from the untreated control group.

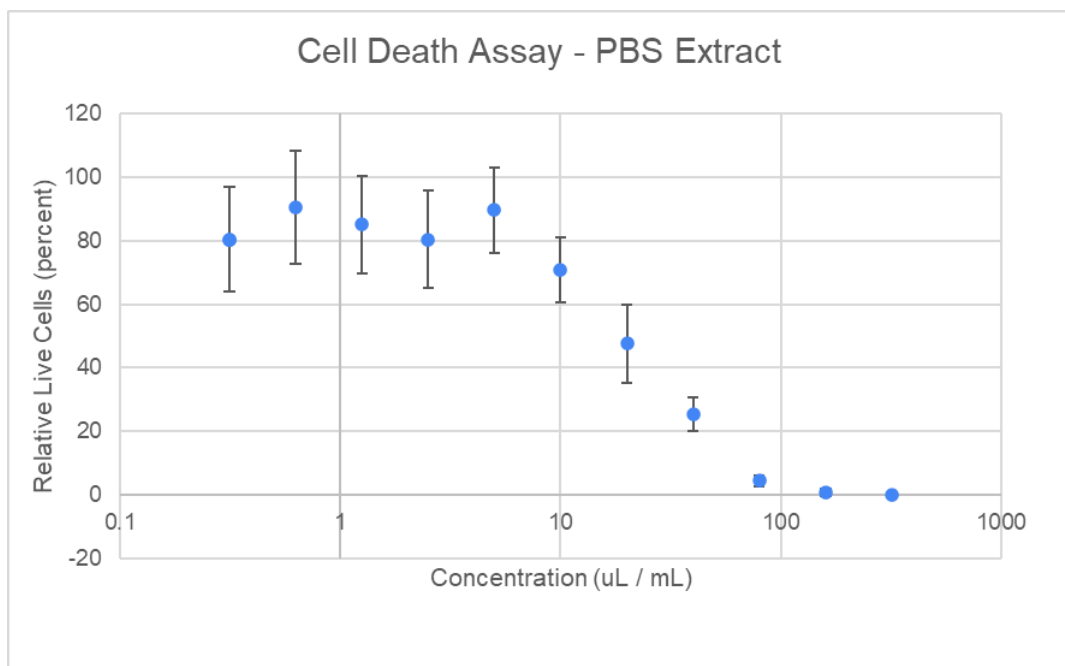


Figure 9. Cell Death Assay - PBS Extract

A cell death curve of HEK293 cells treated with the combined PBS extract. A trendline is given by the equation $y = -31.1\ln(x) + 140.8$. The LD50 value is 18.5 $\mu\text{L} / \text{mL}$. Relative live cells was calculated by dividing the number of live cells from the untreated control group.

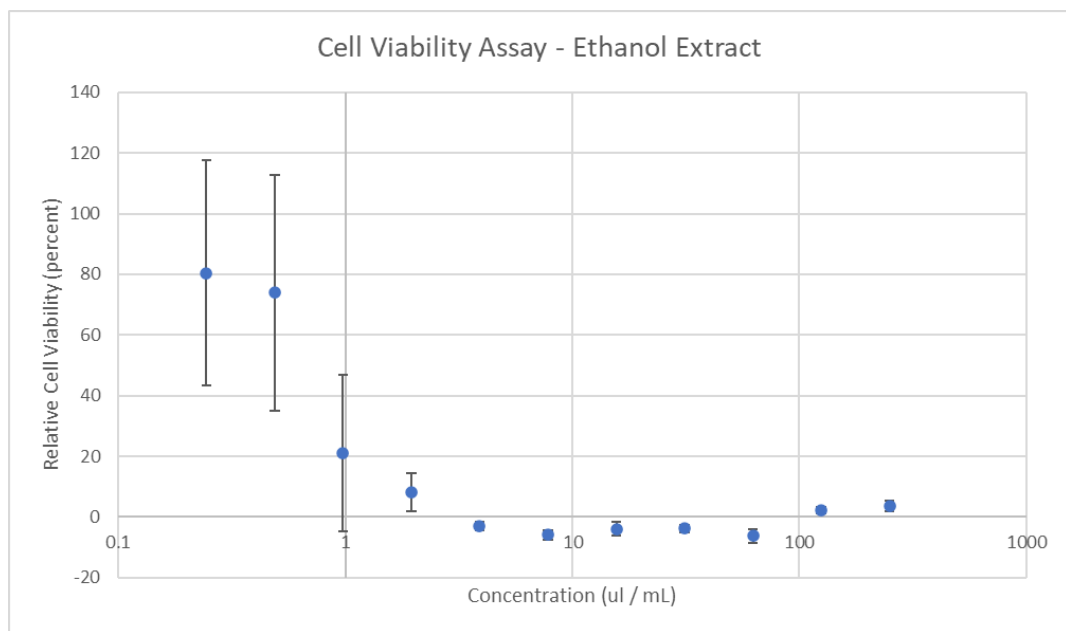


Figure 10. Cell Viability Assay - Ethanol Extract

A cell viability curve of HEK293 cells treated with the combined ethanol extract. A trendline is given by the equation $y = -38.92\ln(x) + 31.468$. The LD50 value is $0.62 \mu\text{L} / \text{mL}$. Relative cell viability was calculated by dividing the absorbance reading at 570 nm of the sample by absorbance reading of the untreated control group.

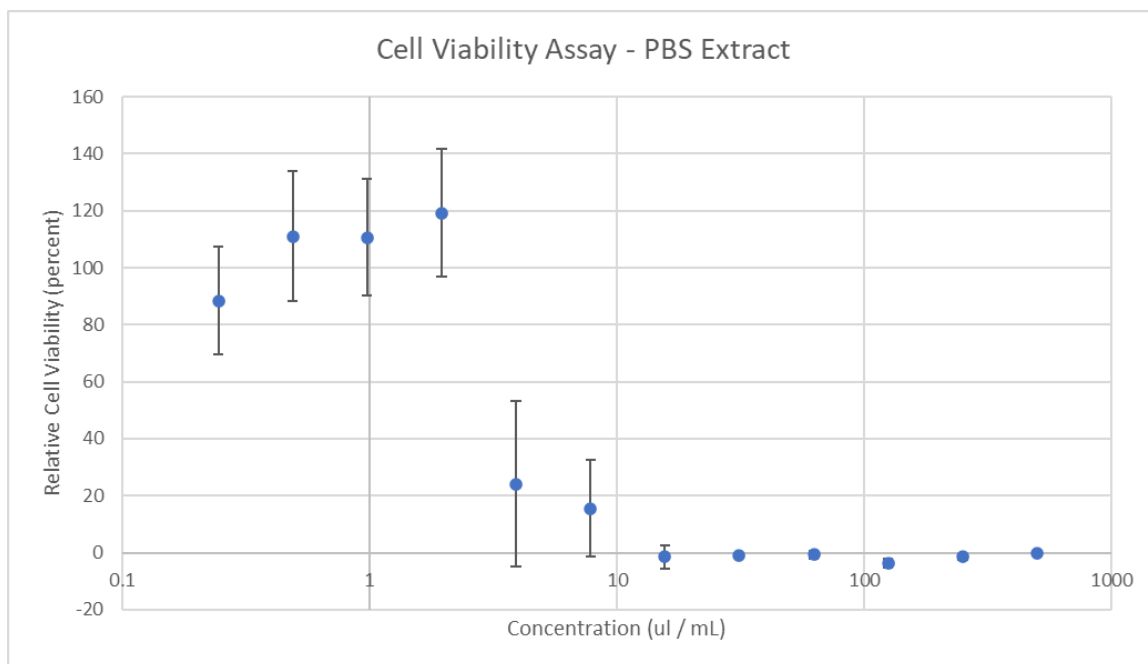


Figure 11. Cell Viability Assay - PBS Extract

A cell viability curve of HEK293 cells treated with the combined PBS extract. A trendline is given by the equation $y = -54.89\ln(x) + 123.15$. The LD50 value is 3.79 $\mu\text{L} / \text{mL}$. Relative cell viability was calculated by dividing the absorbance reading at 570 nm of the sample by absorbance reading of the untreated control group.

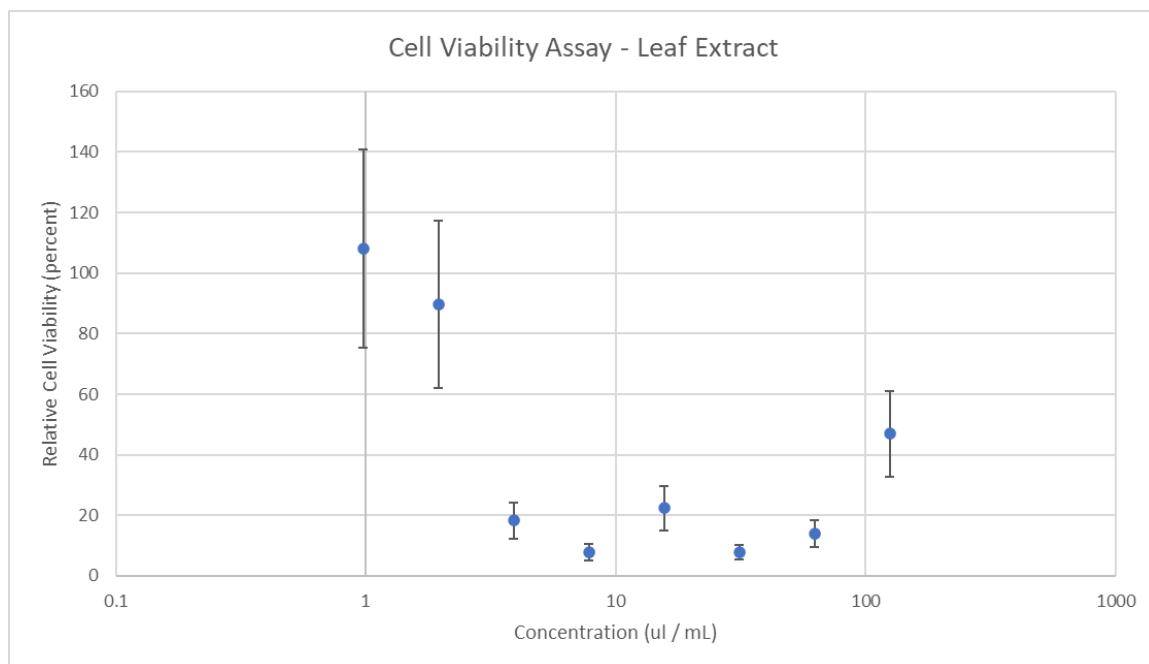


Figure 12. Cell Viability Assay - Leaf Extract

A cell viability curve of HEK293 cells treated with the leaf extract. A trendline is given by the equation $y = -53.72\ln(x) + 110.55$. The LD50 value is 3.09 $\mu\text{l} / \text{mL}$. Relative cell viability was calculated by dividing the absorbance reading at 570 nm of the sample by absorbance reading of the untreated control group.

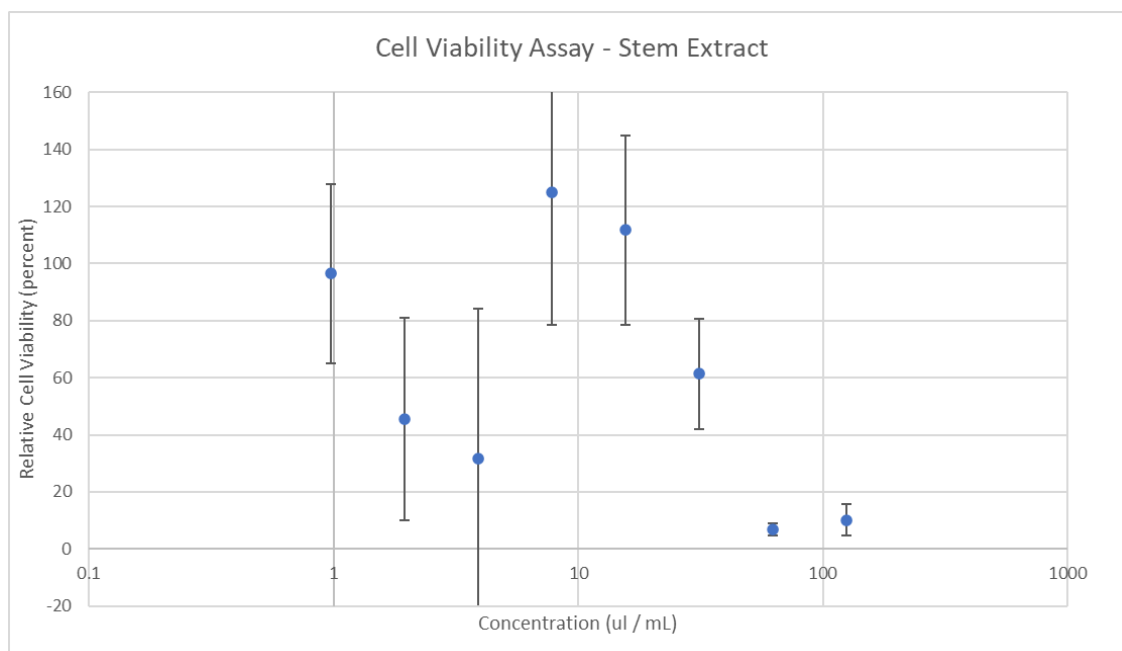


Figure 13. Cell Viability Assay - Stem Extract

A cell viability curve of HEK293 cells treated with the stem extract. A trendline is given by the equation $y = -58.41\ln(x) + 257.02$. The LD50 value is 34.61 $\mu\text{l} / \text{mL}$. Relative cell viability was calculated by dividing the absorbance reading at 570 nm of the sample by absorbance reading of the untreated control group.

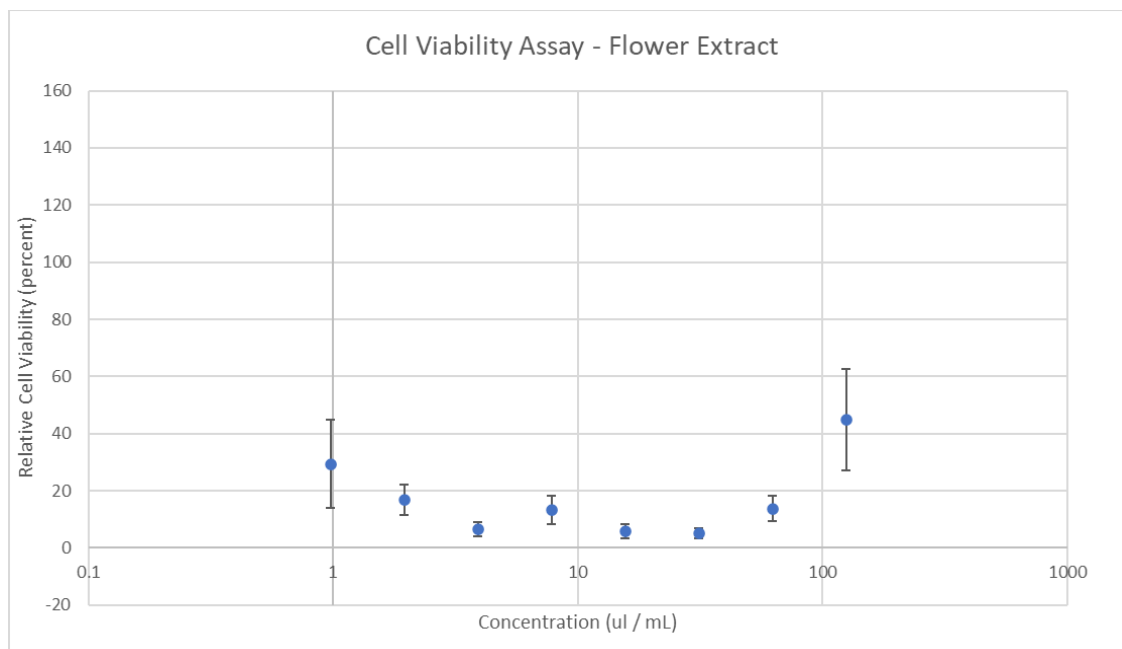


Figure 14. Cell Viability Assay - Flower Extract

A cell viability curve of HEK293 cells treated with the flower extract. A trendline is given by the equation $y = -16.52\ln(x) + 28.61$. The LD50 value is 0.27 $\mu\text{l} / \text{mL}$. Relative cell viability was calculated by dividing the absorbance reading at 570 nm of the sample by absorbance reading of the untreated control group.

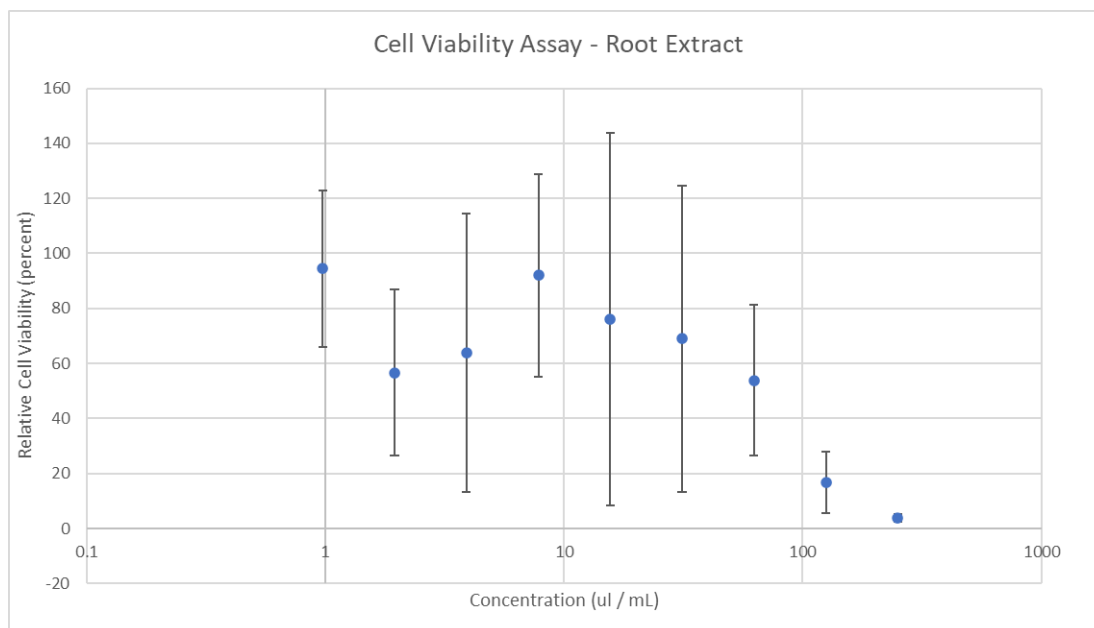


Figure 15. Cell Viability Assay - Root Extract

A cell viability curve of HEK293 cells treated with the root extract. A trendline is given by the equation $y = -33.54\ln(x) + 186.21$. The LD50 value is 58.0 $\mu\text{L} / \text{mL}$. Relative cell viability was calculated by dividing the absorbance reading at 570 nm of the sample by absorbance reading of the untreated control group.

HPLC for Sesquiterpene Lactone Identification

HPLC was run on a methanol gradient at 1 mL / minute through a solid phase silicon column. The chromatograms give the retention time in minutes on the x-axis and the intensity on the y-axis. Helenalin at a concentration of 10 nM was run through the column first to determine the retention time of a model sesquiterpene lactone. The retention time was 17.0 minutes (Table 7) and we were able to observe a clean peak (Figure 22). There were two minor increases in absorbance which were below the threshold for the software to identify them

as peaks. This could be due to sample degradation over time. Care was taken to keep Helenalin stored at 4°C, however during HPLC it is not possible to prevent the sample from sitting at room temperature for several hours before injection.

The chromatogram of the combined ethanol extract has a large number of peaks at various retention times, which was expected in a sample directly extracted from a plant (Figure 17). The retention times closest to 17 minutes are given in Table 2, and it includes a peak at 17.2 minutes. For the combined PBS extract, the chromatogram is very similar but with a few peaks absent from the ethanol extract (Figure 16). This was expected, because the PBS extract was a resuspension of the fully evaporated ethanol extract, and it is likely that not all of the compounds were water soluble. The PBS extract had a peak at 17.3, which is likely the same compound as the 17.2 peak from the ethanol extract (Table 1).

The chromatograms of the leaf, stem, flower, and root extracts are given in figures 18, 19, 20, and 21 respectively. The leaf and flower extracts had the higher number of overall peaks, indicating that a larger number of compounds are present in the extract. The stem had a much lower number of peaks, and the roots had the fewest peaks of all. Among the peaks closest to a 17 minute retention time, the leaf extract had peaks at 16.7 and 17.2 which could be sesquiterpene lactones (Table 3). The stem extract had a peak around 17.5 (Table 4). The flower extract had a 17.1 retention time which was the closest peak to the 17.0 time of Helenalin and the 17.2/17.3 value observed in the

combined ethanol/PBS extract (Table 5). The root extract is very unlikely to contain sesquiterpene lactones similar to Helenalin, and the peak closest to 17 minutes had a retention time of 15.5 minutes (Table 6).

Finally, we compared the Photodiode array detector (PDA) data which measures the spectral profiles of the compounds as they exit the column. This is given in Figure 28. Helenalin has a clear absorbance around 220-230 nm. The combined ethanol extract shows a similar absorbance pattern between 220-230 nm as well as a second absorbance around 330 nm. This is also true for the PBS extract however the signal intensity is much lower.

The leaf extract shows a strong absorbance in the 17.2 minute peak between 220 and 230 nm, along with another absorbance at 270 nm and a third at 340 nm. Interestingly, the 17.6 minute peak shows a similar pattern suggesting that it could be a highly similar compound. The flower extract has a pattern similar to the combined ethanol extract. The 17.1 minute peak has an absorbance around 220 - 230 nm as well as another peak around 330 nm. The stem and root extracts do not show a significant increase in absorbance between 220 to 400 nm within 16.5 to 18.0 minutes.

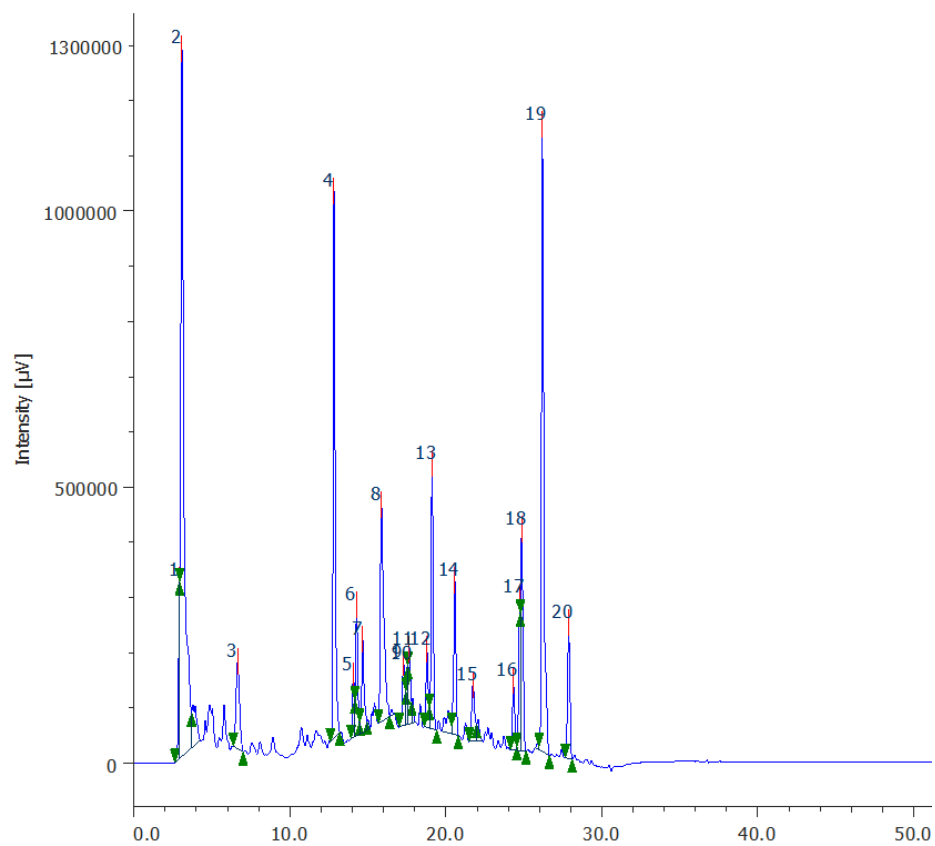


Figure 16. HPLC Chromatogram - PBS Extract

Peak Number	Retention Time	Area	Height
8	15.9	6100509	391487
9	17.3	1409167	112608
10	17.5	692619	108044
11	17.6	1471466	133981
12	18.8	1314564	1314564

Table 1. HPLC Chromatogram Peaks - PBS Extract

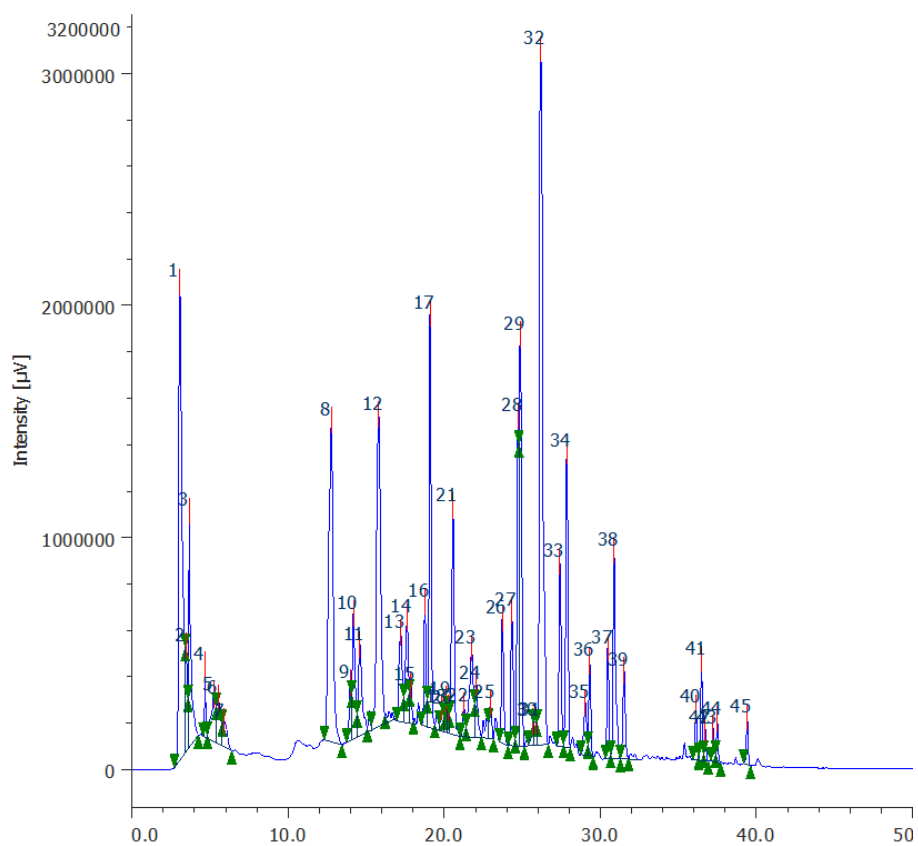


Figure 17. HPLC Chromatogram - Ethanol Extract

Peak Number	Retention Time	Area	Height
12	15.8	25283344	1343839
13	17.2	5652009	384417
14	17.6	6234405	454204
15	17.8	1422956	164814
16	18.8	4893308	533620

Table 2. HPLC Chromatogram Peaks - Ethanol Extract

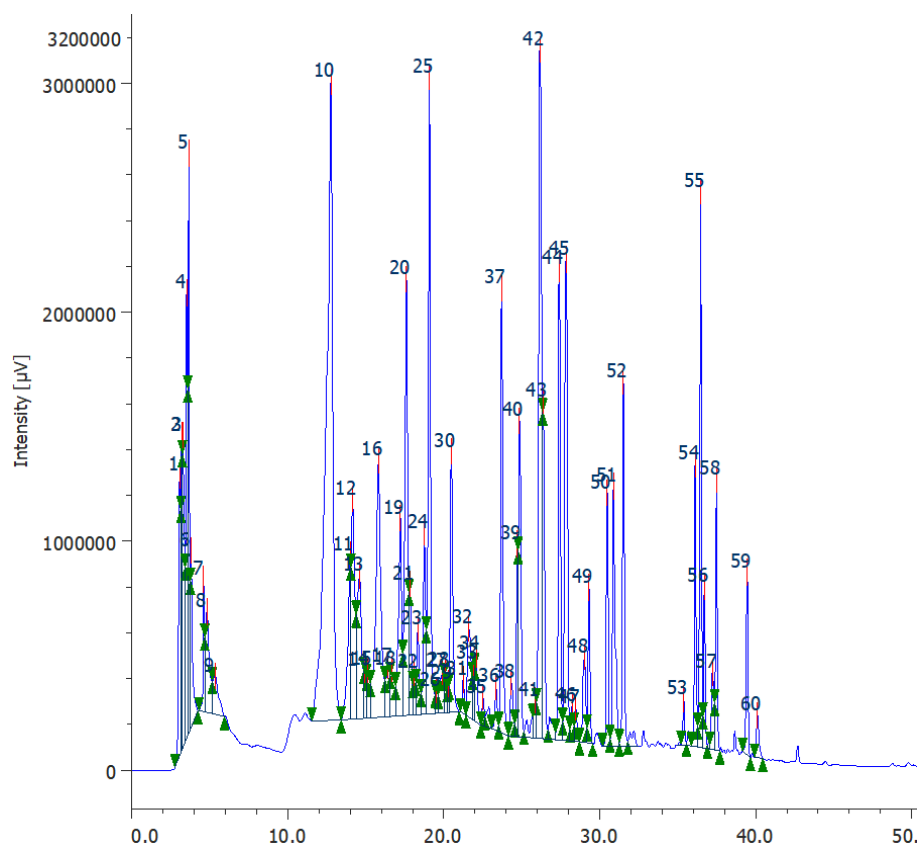


Figure 18. HPLC Chromatogram - Leaf Extract

Peak Number	Retention Time	Area	Height
17	16.4	3882411	222290
18	16.7	3781468	207764
19	17.2	12438193	862638
20	17.6	24675666	1904111
21	17.8	4979929	571357

Table 3. HPLC Chromatogram Peaks - Leaf Extract

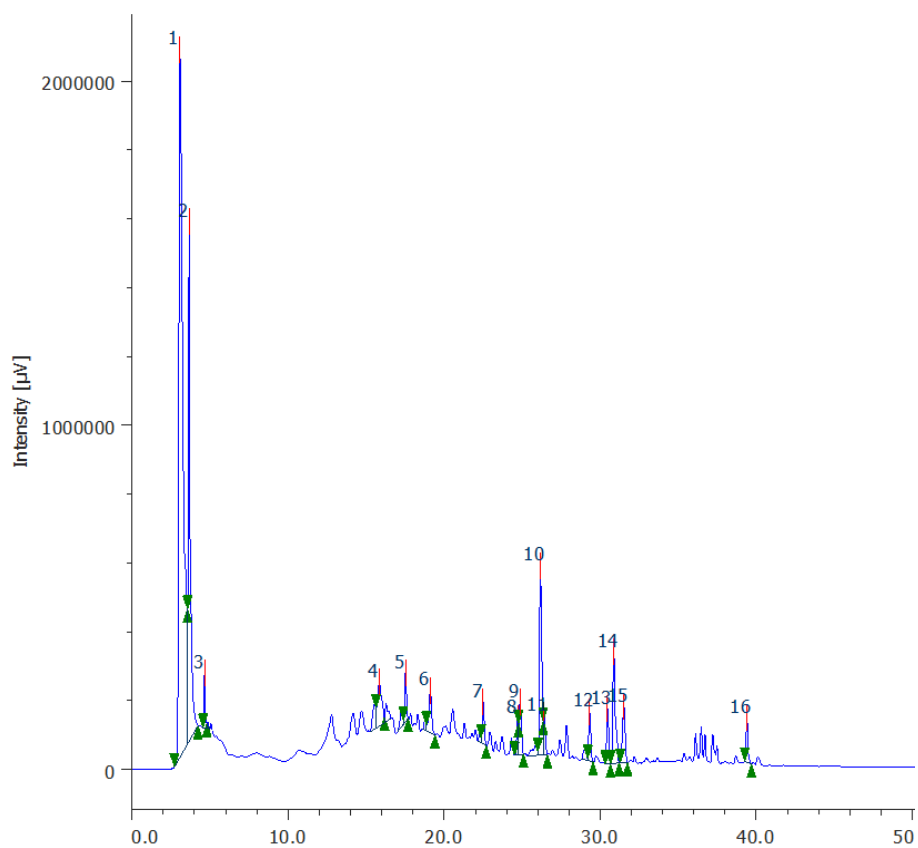


Figure 19. HPLC Chromatogram - Stem Extract

Peak Number	Retention Time	Area	Height
4	15.8	2484429	126840
5	17.5	1174111	141642
6	19.1	1478118	122660
7	22.5	1099265	120413
8	24.7	842481	106917

Table 4. HPLC Chromatogram Peaks - Stem Extract

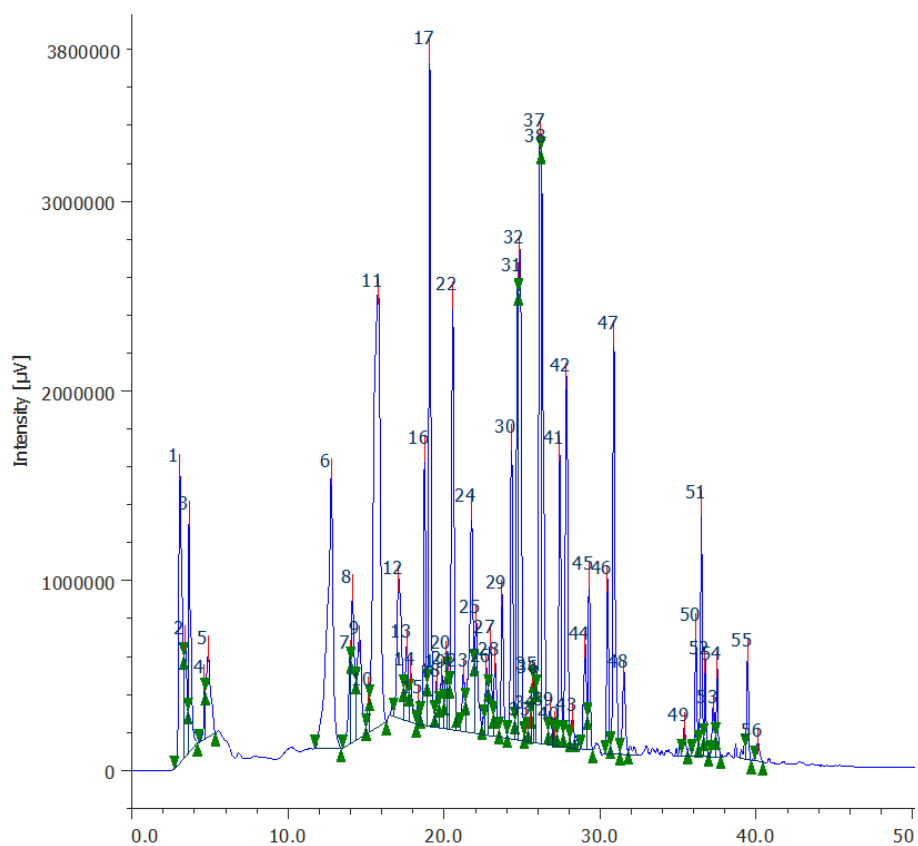


Figure 20. HPLC Chromatogram - Flower Extract

Peak Number	Retention Time	Area	Height
13	15.8	67836720	2290065
14	17.1	15044572	733753
15	17.6	5763036	416595
16	17.8	3244758	273911
17	18.3	1327104	141251

Table 5. HPLC Chromatogram Peaks - Flower Extract

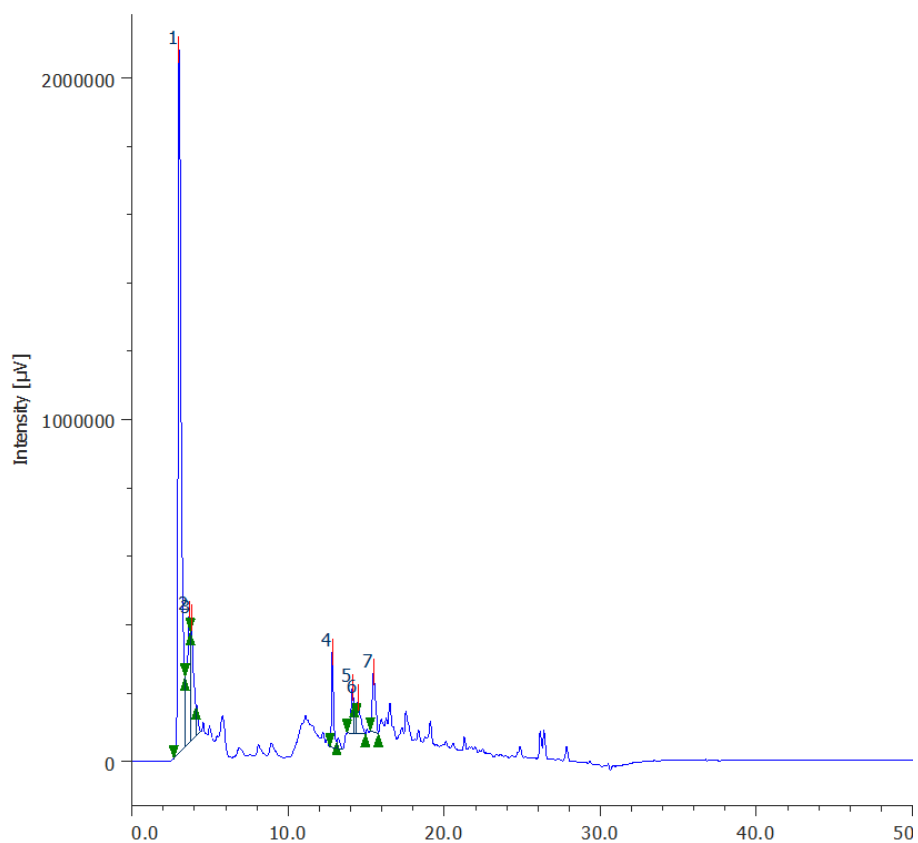


Figure 21. HPLC Chromatogram - Root Extract

Peak Number	Retention Time	Area	Height
3	3.80	4901489	358364
4	12.8	2497550	280310
5	14.1	1678986	134253
6	14.5	1541767	102840
7	15.5	2458587	175633

Table 6. HPLC Chromatogram Peaks - Root Extract

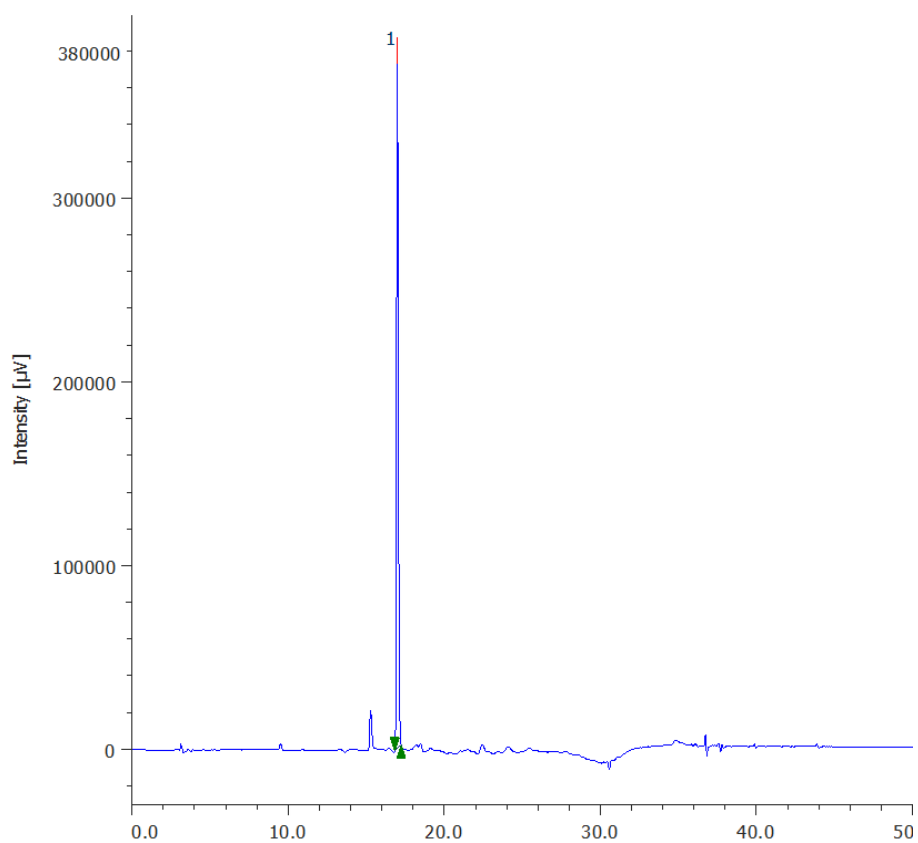


Figure 22. HPLC Chromatogram - Helenalin Standard

Et	Retention Time	Area	Height
1	17.0	2996422	380021

Table 7. HPLC Chromatogram Peaks - Helenalin Standard

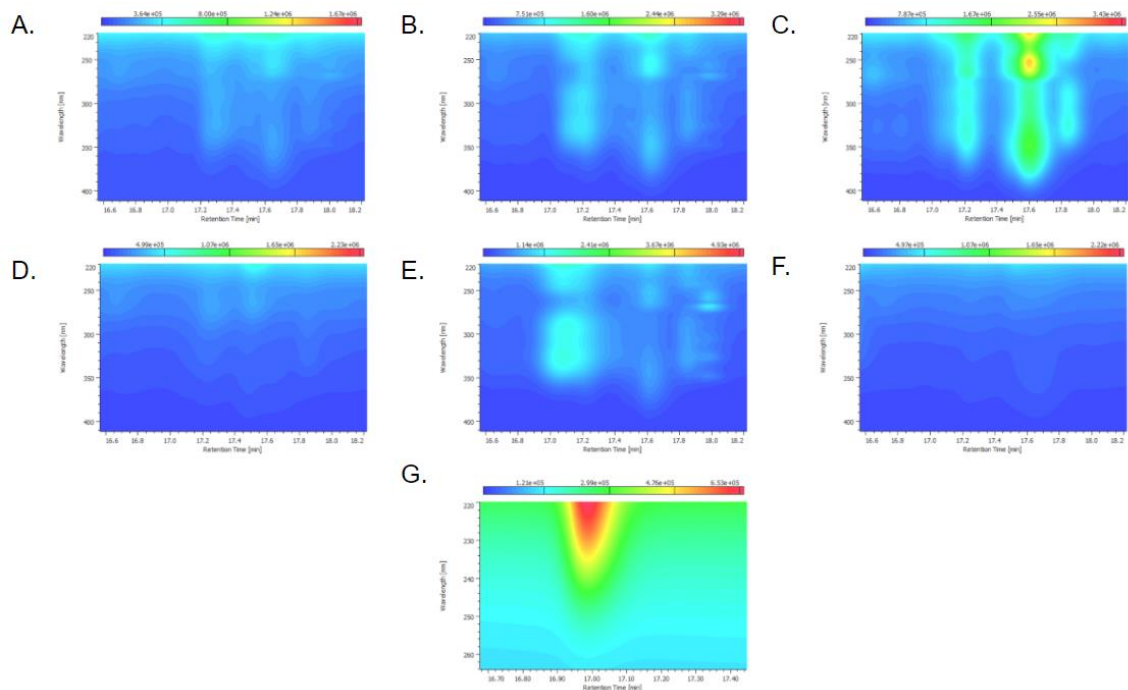


Figure 23. HPLC Chromatogram - Comparative Absorbance Spectra of RT 17 Peak

Inflammation Assay and Differential Gene Expression

The results of the RNA sequencing were sent from Novogene as FASTQ files; however, the purity and integrity of the RNA was compromised during the shipping process. Following the processing of the RNA data into a count matrix which was used to run DeSEQ2, we constructed volcano plots using the only tool VolcaNoseR (68). Evidence of apoptosis was determined by the presence of upregulated pro-apoptotic genes given by the Kyoto Encyclopedia of Genes and Genomics (KEGG) pathway for Apoptosis (69). Evidence of NF- κ B induced gene

upregulation was determined by the presence of upregulated NF- κ B related genes (70).

For the differential expression of the PBS Extract pretreated sample vs. the control, we see no evidence of apoptosis (Figure 24, Table 8). There are only two genes from the KEGG apoptosis pathway that were significantly upregulated. BID is a member of the BCL-2 protein family and an apoptosis regulator that can heterodimerize with BAX to mediate mitochondrial damage (71). PMAIP1 is also a member of the BCL-2 protein family and inhibits the anti-apoptotic BCL-2 members (72). We see a large amount of significant upregulation and downregulation of thousands of genes between these two samples.

Comparing the gene expression of TNF- α treated cells vs. the control (Figure 25, Table 9), we see no evidence of NF- κ B induced gene upregulation. Out of the 16 genes we searched for, only CXCL1 was significantly upregulated. CXCL1 is a chemokine that acts as an attractant for immune cells when expressed by the host (73). For the Extract / TNF- α treated cells vs. the control (Figure 26, Table 10), and the Extract / TNF- α treated cells vs. TNF- α (Figure 27, Table 11) we also see no evidence of upregulation or downregulation in NF- κ B induced gene expression. CXCL1 is again the only significantly upregulated gene between the Extract / TNF- α treated cells vs. the control.

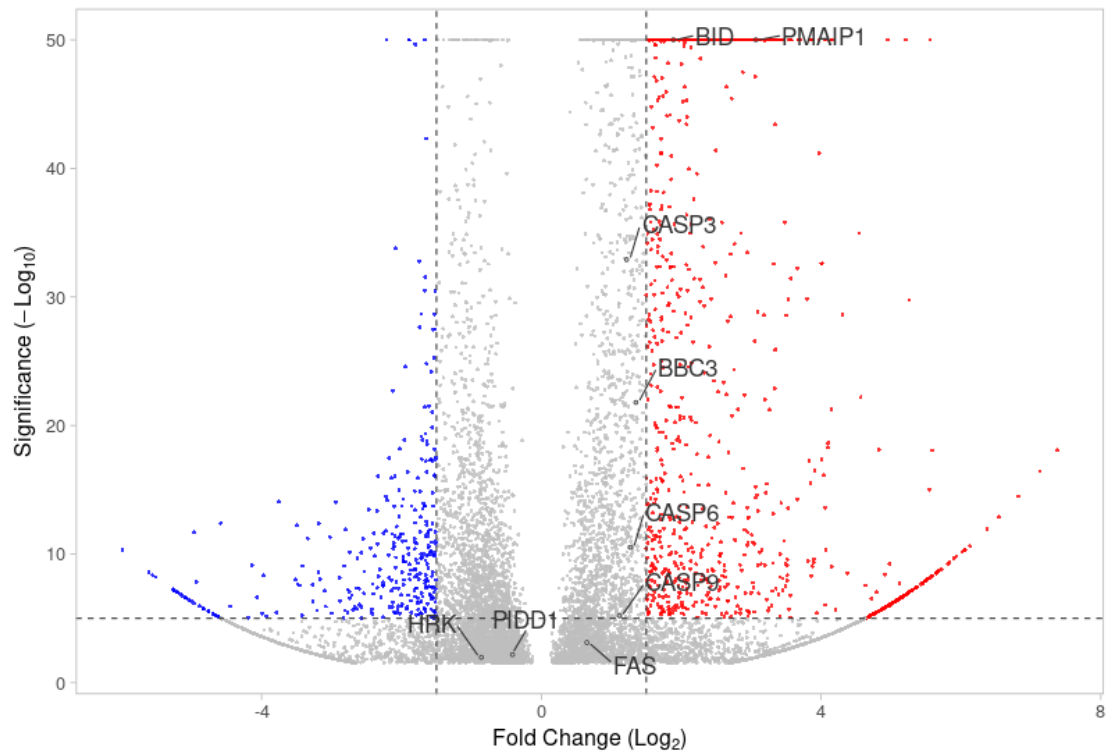


Figure 24. Volcano plot PBS extract vs. Control

Gene	Change	Log2(Fold Change)	Log10(p-value)
PMAIP1	Increased	3.066811	50
BID	Increased	1.887706	50
CASP3	Unchanged	1.21883	32.90234
BBC3	Unchanged	1.351967	21.79366
CASP6	Unchanged	1.275283	10.52407
CASP9	Unchanged	1.115456	5.204142
FAS	Unchanged	0.651142	3.114098
PIDD1	Unchanged	-0.41318	2.17432
HRK	Unchanged	-0.85842	1.966567

Table 8. Differentially Expressed genes for PBS Extract vs. Control

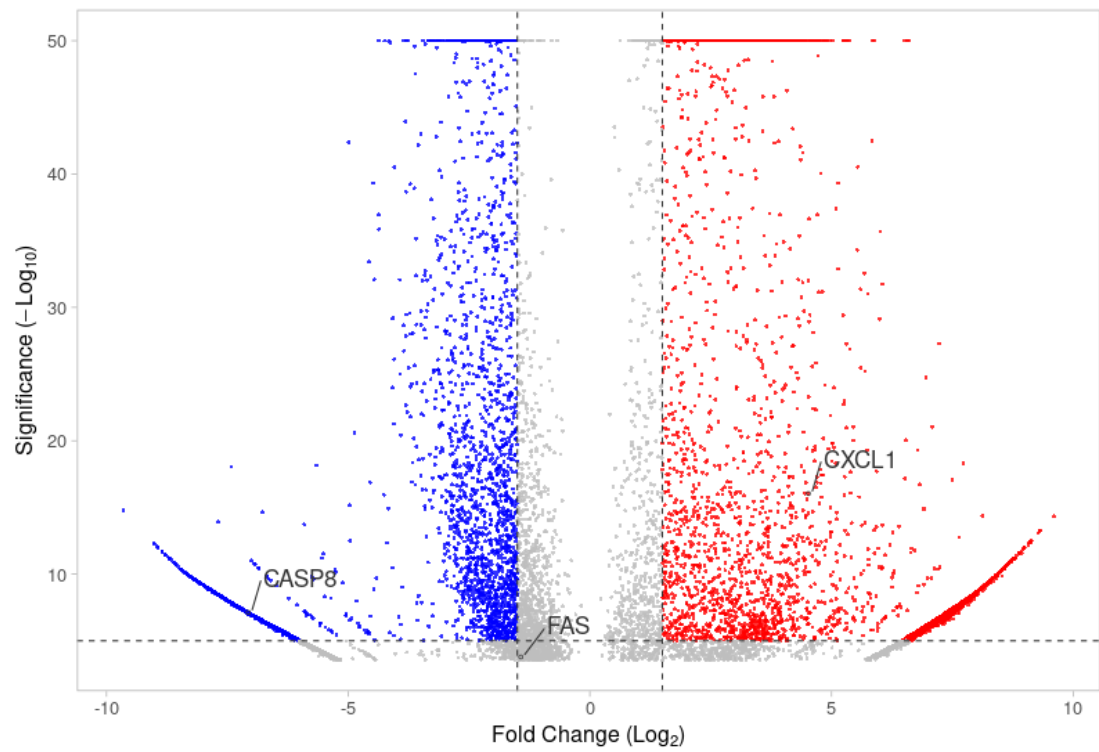


Figure 25. Volcano plot TNF- α vs. Control

Gene	Change	Log2(Fold Change)	Log10(p-value)
CXCL1	Increased	4.521707	16.03787
CASP8	Decreased	-7.06875	7.125812
FAS	Unchanged	-1.42827	3.785233
CFLAR	Unchanged	0.04822	0.042152
BCL2	Unchanged	0.052332	0.00972
CASP10	Unchanged	0.707377	1.126532
IL1A	Unchanged	0	0
IL2	Unchanged	0	0
IL6	Unchanged	0	0
IL12A	Unchanged	1.324944	1.668349
TNF	Unchanged	0	0
CCL2	Unchanged	0	0
CXCL10	Unchanged	0	0
ICAM1	Unchanged	3.845783	2.915562
VCAM1	Unchanged	-0.54661	0

Table 9. Differentially expressed genes for TNF- α vs. Control

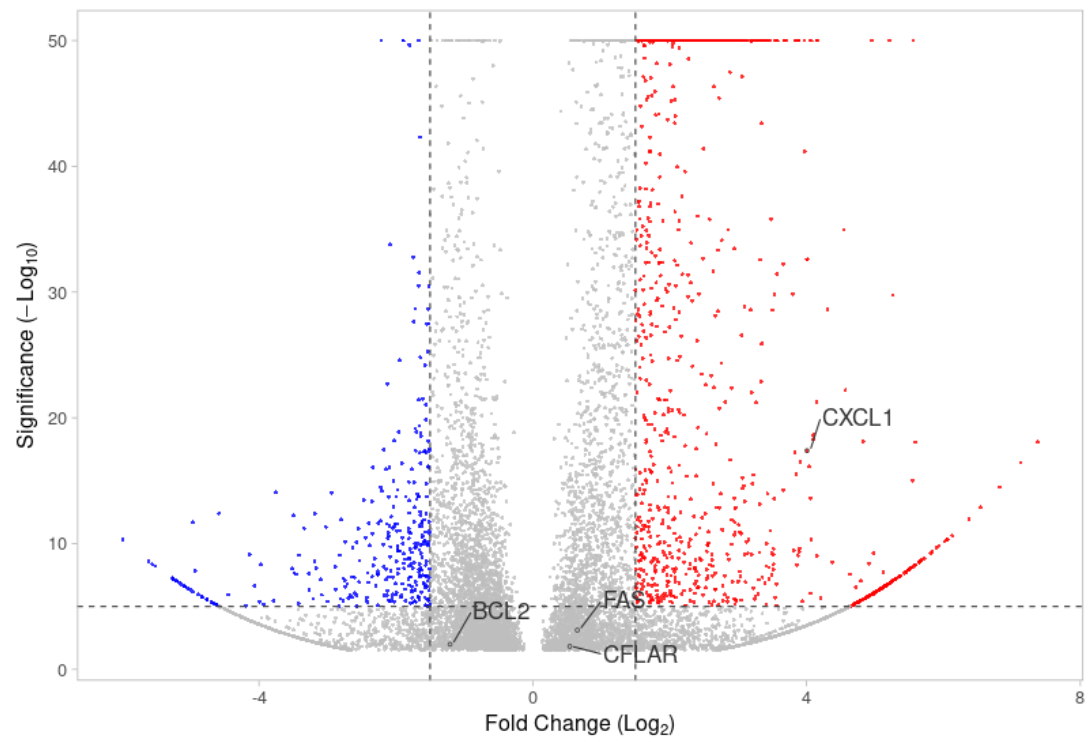


Figure 26. Volcano plot PBS extract / TNF- α vs. Control

Gene	Change	Log2(Fold Change)	Log10(p-value)
CXCL1	Increased	4.006334	17.38704
FAS	Unchanged	0.651142	3.114098
BCL2	Unchanged	-1.2088	1.990282
CFLAR	Unchanged	0.540431	1.825198
CASP8	Unchanged	0.359798	1.040113
CASP10	Unchanged	0.087144	0.078977
IL1A	Unchanged	0	0
IL2	Unchanged	0	0
IL6	Unchanged	0	0
IL12A	Unchanged	1.06794	1.358528
TNF	Unchanged	0	0
CCL2	Unchanged	0	0
CXCL10	Unchanged	0.533262	0
ICAM1	Unchanged	1.25505	0.565746
VCAM1	Unchanged	0.334792	0.094653

Table 10. Differentially expressed genes for PBS Extract / TNF- α vs. Control

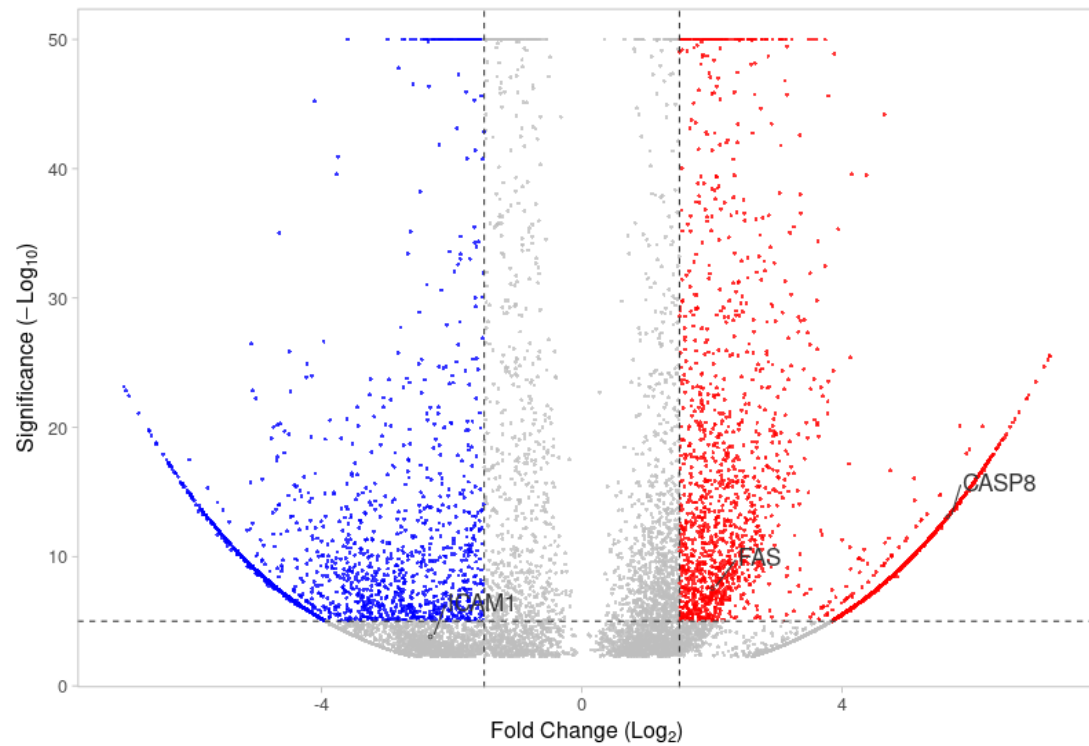


Figure 27. Volcano plot PBS extract / TNF- α vs. TNF- α treatment

Gene	Change	Log2(Fold Change)	Log10(p-value)
CASP8	Increased	5.623048	13.09146
FAS	Increased	2.002067	7.532523
ICAM1	Unchanged	-2.32635	3.800063
CXCL1	Unchanged	-0.42469	0.624252
BCL2	Unchanged	-0.39112	0.174443
CFLAR	Unchanged	0.466764	0.647494
CASP10	Unchanged	-0.60186	0.718095
IL1A	Unchanged	0	0
IL2	Unchanged	0	0
IL6	Unchanged	0	0
IL12A	Unchanged	-0.22538	0.158
TNF	Unchanged	0	0
CCL2	Unchanged	0	0
CXCL10	Unchanged	0.131093	0
VCAM1	Unchanged	0.313941	0

Table 11. Differentially expressed genes for PBS extract vs. TNF- α treatment

CONCLUSION

Eupatorium serotinum was identified in the field based on morphological characteristics. The species of the sample was confirmed at a herbarium to be *E. serotinum*. A crude ethanol extraction in which the plant material was divided by segments into jars filled with ethanol was successful at extracting compounds which could include sesquiterpene lactones. Further filtering and evaporation of excess ethanol allowed us to concentrate the extractions. An ethanol-free compound suspended in PBS was also made, although many of the compounds that were present in the ethanol extraction did not appear soluble in water.

The cytotoxicity of the extracts given by LD50 was determined by two different assays. In the cell death assay, the LD50 for the combined ethanol and PBS extracts was determined by counting the number of live cells following treatment with different concentrations of the extract. In the cell viability test, the LD50 was determined by measuring the metabolic activity of the cells compared with an untreated control. The LD50 values determined by the cell death assay are around 5 times higher than the LD50 values from the cell viability assay. This is reasonable, and it can be concluded that many of the cells with very low metabolic activity due to treatment would still be considered “living” cells in the

cell death assay. For this reason, the cell viability assay will always give a higher estimate of cytotoxicity.

In both cases, the combined ethanol extract was around 4 times more toxic than the combined PBS extract. This difference is unlikely to be due to the toxic effects of ethanol, as the root extract was also ethanol based, and was over 15 times less toxic than the PBS extract. Among the extracts from the different plant segments, there is a large difference in cytotoxicity. The root extract is the least toxic followed by the stem extract. The leaf extract is nearly as toxic as the PBS extract. Interestingly, the flower extract is the most toxic of all samples. It is twice as toxic as the combined ethanol extract and over 2,000 times more toxic than the root extract.

From the HPLC results, it can be concluded that the combined ethanol extract and the combined PBS extract are very similar in composition. The only differences are a few peaks which are either absent or peaks which are much smaller in the PBS extract than in the ethanol extract. It can be concluded that these compounds were water-insoluble, and any future attempts to extract and purify those peaks should be done in an ethanol solution. Both of the combined extracts showed peaks at 17.2/17.3 minutes, which is close to the retention time of Helenalin. On the PDA, both peaks correspond to the 220 - 230 nm absorbance of Helenalin, however they also had an absorbance value at 330 nm. SLs are a diverse class of compounds, which can be modified in many different

ways. Though we wouldn't expect minor modification to significantly change the retention time, modified SLs would have changes in their absorbance spectra. It is likely that the peak at 17.2/17.3 from the ethanol extraction and PBS extraction respectively are modified SLs.

Sesquiterpene lactones are most likely present in the flowers and leaves, as opposed to the stems and roots. Among the chromatograms of the individual plant segments, we see very few peaks from the root extract, with no peak around 17 minutes. We can conclude that very few compounds were extracted in ethanol from the roots. Future studies on the roots should try different extraction methods. The stem extract had the second fewest peaks, although it did have a peak around 17.5. This could be a modified SL, as the PDA shows a similar absorbance at 220 - 230 nm. Both the flower extract and the leaf extract have strong peaks around 17 minutes. The leaf extract has two peaks around that point which both have identical absorbances to the combined extracts. These could be highly similar SLs, with only minor changes having an effect on retention time rather than absorbance. Finally, the flower extract has a peak with a retention time closest to helenalin at 17.1 minutes. The absorbance spectrum also has the typical pattern of an absorbance around 220 - 230 nm and a second absorbance around 330 nm.

In order to confirm that these peaks are sesquiterpene lactones, future studies should collect fractions of the extract as they exit the column. Sub

fractionalization should then be performed until the solution contains a majority species. This majority species could then be analyzed by NMR to get a molecular structure. The data generated by this project suggests that multiple peaks discovered in these chromatograms could be modified SLs.

The differential gene expression analysis was potentially compromised by the poor-quality RNA we extracted following the inflammation assay. The RNA likely degraded during the delayed shipping process and affected our results. We saw no evidence of apoptosis between the samples treated with our PBS Extract and the control. This was expected, as we treated our cells with a non-toxic concentration of our extract as determined by the cytotoxicity assays. The TNF- α treated cells did not show significant upregulation of NF- κ B induced genes with the exception of the pro-apoptotic CXCL1. This was not expected, as the TNF- α treated cells were expected to show a strong upregulation in NF- κ B induced genes as a part of an inflammation response. There was also no change in NF- κ B induced gene expression between the Extract-pretreated / TNF- α treated cells vs. the TNF- α treated cells. This does not necessarily mean that the SLs in our Extract were not effective; these results are likely due to RNA degradation either during shipping or poor RNA extraction.

Going forward, we hope to collect more samples of *E. serotinum* for extraction. It would be prudent to sample from multiple sites across its entire habitat, in order to test for any local variation in SL production or toxicity. With

enough plant mass from which to extract, we would be able to fractionalize the extractions with column chromatography and HPLC in order to isolate the possible SL compounds from *E. serotinum*. Nuclear magnetic resonance (NMR) spectroscopy could be employed to determine the molecular structure of the isolated SLs. Cytotoxicity and anti-inflammatory properties could be determined using the techniques outlined previously. Should an SL be discovered with anti-inflammatory potential and a low cytotoxicity, it would represent a promising new drug for the treatment of chronic inflammation.

REFERENCES

1. World Health Organization (2019) *WHO Global Report on Traditional and Complementary Medicine 2019*, World Health Organization
2. Peltzer, K., and Pengpid, S. (2018) Prevalence and Determinants of Traditional, Complementary and Alternative Medicine Provider Use among Adults from 32 Countries. *Chin. J. Integr. Med.* **24**, 584–590
3. Barnes, P. M., Bloom, B., and Nahin, R. L. (2008) Complementary and alternative medicine use among adults and children: United States, 2007. Natl. Health Stat. Report.
4. Hay, M., Thomas, D. W., Craighead, J. L., Economides, C., and Rosenthal, J. (2014) Clinical development success rates for investigational drugs. *Nat. Biotechnol.* **32**, 40–51
5. Tu, Y. (2011) The discovery of artemisinin (qinghaosu) and gifts from Chinese medicine. *Nat. Med.* **17**, 1217–1220
6. White, N. J. (2008) Qinghaosu (artemisinin): the price of success. *Science.* **320**, 330–334
7. Shimizu, K., Funamoto, M., Sunagawa, Y., Shimizu, S., Katanasaka, Y., Miyazaki, Y., Wada, H., Hasegawa, K., and Morimoto, T. (2019) Anti-inflammatory Action of Curcumin and Its Use in the Treatment of Lifestyle-related Diseases. *Eur Cardiol.* **14**, 117–122
8. Oketch-Rabah, H. A., Marles, R. J., Jordan, S. A., and Low Dog, T. (2019) United States Pharmacopeia Safety Review of Willow Bark. *Planta Med.* **85**, 1192–1202

9. Colegate, S. M., Upton, R., Gardner, D. R., Panter, K. E., and Betz, J. M. (2018) Potentially toxic pyrrolizidine alkaloids in *Eupatorium perfoliatum* and three related species. Implications for herbal use as boneset. *Phytochem. Anal.* **29**, 613–626
10. Sugumar, N., Karthikeyan, S., and Gowdhami, T. Chemical composition and antimicrobial activity of essential oil from *Eupatorium triplinerve* Vahl. Aerial parts. [online] <https://bibliotekanauki.pl/articles/10855.pdf> (Accessed April 14, 2023)
11. Judzentiene, A., Garjonyte, R., and Budiene, J. (2016) Variability, toxicity, and antioxidant activity of *Eupatorium cannabinum* (hemp agrimony) essential oils. *Pharm. Biol.* **54**, 945–953
12. Gao, T., Yao, H., Song, J., Zhu, Y., Liu, C., and Chen, S. (2010) Evaluating the feasibility of using candidate DNA barcodes in discriminating species of the large Asteraceae family. *BMC Evol. Biol.* **10**, 324
13. Panero, J., and Funk, V. A. (2002) Toward a phylogenetic subfamilial classification for the Compositae (Asteraceae). *Proceedings of the Biological society of Washington*
14. Hodálová, I., Lansdown, R., and Petrova, A. (2023) Arnica Montana. in *LiverTox: Clinical and Research Information on Drug-Induced Liver Injury*, National Institute of Diabetes and Digestive and Kidney Diseases, Bethesda (MD)
15. Bruelheide, H., and Scheidel, U. (1999) Slug herbivory as a limiting factor for the geographical range of *Arnica montana*. *J. Ecol.* **87**, 839–848
16. Waizel-Bucay, J., and Cruz-Juárez, M. de L. (2014) *Arnica montana* L., relevant European medicinal plant. *Revista mexicana de ciencias forestales.* **5**, 98–109

17. Luijten, S. H., Oostermeijer, J. G. B., van Leeuwen, N. C., and den Nijs, H. C. M. (1996) Reproductive success and clonal genetic structure of the rare *Arnica montana* (Compositae) in The Netherlands. *Plant Syst. Evol.* **201**, 15–30
18. Sugier, D., Sugier, P., and Gawlik-Dziki, U. (2013) Propagation and introduction of *Arnica montana* L. into cultivation: a step to reduce the pressure on endangered and high-valued medicinal plant species. *ScientificWorldJournal.* **2013**, 414363
19. Aiello, N., Bontempo, R., Vender, C., Ferretti, V., Innocenti, G., and Dall'Acqua, S. (2012) Morpho-quantitative and qualitative traits of *Arnica montana* L. wild accessions of Trentino, Italy. *Ind. Crops Prod.* **40**, 199–203
20. Galambosi, B. (2004) Introduction of *Arnica montana* L. in Finland
21. Zhang, M.-L., Wu, M., Zhang, J.-J., Irwin, D., Gu, Y.-C., and Shi, Q.-W. (2008) Chemical constituents of plants from the genus *Eupatorium*. *Chem. Biodivers.* **5**, 40–55
22. Tabanca, N., Bernier, U. R., Tsikolia, M., Becnel, J. J., Sampson, B., Werle, C., Demirci, B., Başer, K. H. C., Blythe, E. K., Pounders, C., and Wedge, D. E. (2010) *Eupatorium capillifolium* essential oil: chemical composition, antifungal activity, and insecticidal activity. *Nat. Prod. Commun.* **5**, 1409–1415
23. Lewis, W. H., and Elvin-Lewis, M. P. F. (2003) *Medical Botany: Plants Affecting Human Health*, John Wiley & Sons, Hoboken, NJ
24. Bohlmann, F., Zdero, C., King, R. M., and Robinson, H. (1985) Further Germacranolides from *Eupatorium serotinum*. *Planta Med.* **51**, 76–77
25. Johnson, M. F. (1974) Eupatorieae (Asteraceae) in Virginia: *Eupatorium* L. *Castanea.* **39**, 205–228

26. Tomley, A. J., and Panetta, F. D. Eradication of the exotic weeds *Helenium amarum* (Rafin) H.L. and *Eupatorium serotinum* Michx. from south-eastern Queensland. [online] <http://caws.org.nz/old-site/awc/2002/awc200212931.pdf> (Accessed April 14, 2023)
27. Medzhitov, R. (2008) Origin and physiological roles of inflammation. *Nature*. **454**, 428–435
28. Aletaha, D., and Smolen, J. S. (2018) Diagnosis and Management of Rheumatoid Arthritis: A Review. *JAMA*. **320**, 1360–1372
29. Rodrigo, G. J., Rodrigo, C., and Hall, J. B. (2004) Acute asthma in adults. *Chest*. **125**, 1081–1102
30. Park, J. H., Peyrin-Biroulet, L., Eisenhut, M., and Shin, J. I. (2017) IBD immunopathogenesis: A comprehensive review of inflammatory molecules. *Autoimmun. Rev.* **16**, 416–426
31. Kawai, T., and Akira, S. (2010) The role of pattern-recognition receptors in innate immunity: update on Toll-like receptors. *Nat. Immunol.* **11**, 373–384
32. Zindel, J., and Kubes, P. (2020) DAMPs, PAMPs, and LAMPs in Immunity and Sterile Inflammation. *Annu. Rev. Pathol.* **15**, 493–518
33. Kumar, H., Kawai, T., and Akira, S. (2009) Toll-like receptors and innate immunity. *Biochem. Biophys. Res. Commun.* **388**, 621–625
34. Pober, J. S. (1998) Activation and injury of endothelial cells by cytokines. *Pathol. Biol.* **46**, 159–163

35. Ghosh, S., May, M. J., and Kopp, E. B. (1998) NF-kappa B and Rel proteins: evolutionarily conserved mediators of immune responses. *Annu. Rev. Immunol.* **16**, 225–260
36. Sun, Z., and Andersson, R. (2002) NF-kB Activation and Inhibition: A Review. *Shock*. **18**, 99
37. Lyss, G., Schmidt, T. J., Merfort, I., and Pahl, H. L. (1997) Helenalin, an anti-inflammatory sesquiterpene lactone from Arnica, selectively inhibits transcription factor NF-kappaB. *Biol. Chem.* **378**, 951–961
38. Ferraz, R. A. C., Lopes, A. L. G., da Silva, J. A. F., Moreira, D. F. V., Ferreira, M. J. N., and de Almeida Coimbra, S. V. (2021) DNA–protein interaction studies: a historical and comparative analysis. *Plant Methods*. **17**, 1–21
39. Singh, J. A., Saag, K. G., Bridges, S. L., Jr, Akl, E. A., Bannuru, R. R., Sullivan, M. C., Vaysbrot, E., McNaughton, C., Osani, M., Shmerling, R. H., Curtis, J. R., Furst, D. E., Parks, D., Kavanaugh, A., O'Dell, J., King, C., Leong, A., Matteson, E. L., Schousboe, J. T., Drevlow, B., Ginsberg, S., Grober, J., St Clair, E. W., Tindall, E., Miller, A. S., and McAlindon, T. (2016) 2015 American College of Rheumatology Guideline for the Treatment of Rheumatoid Arthritis. *Arthritis Rheumatol.* **68**, 1–26
40. Whittle, B. J. (2000) COX-1 and COX-2 products in the gut: therapeutic impact of COX-2 inhibitors. *Gut*. **47**, 320–325
41. Antman, E. M., Bennett, J. S., Daugherty, A., Furberg, C., Roberts, H., Taubert, K. A., and American Heart Association (2007) Use of nonsteroidal antiinflammatory drugs: an update for clinicians: a scientific statement from the American Heart Association. *Circulation*. **115**, 1634–1642
42. Rodriguez, E., Towers, G. H. N., and Mitchell, J. C. (1976) Biological activities of sesquiterpene lactones. *Phytochemistry*. **15**, 1573–1580

43. Merfort, I. (2011) Perspectives on sesquiterpene lactones in inflammation and cancer. *Curr. Drug Targets*. **12**, 1560–1573
44. Hall, I. H., Lee, K. H., Starnes, C. O., Sumida, Y., Wu, R. Y., Waddell, T. G., Cochran, J. W., and Gerhart, K. G. (1979) Anti-inflammatory activity of sesquiterpene lactones and related compounds. *J. Pharm. Sci.* **68**, 537–542
45. Bork, P. M., Schmitz, M. L., Kuhnt, M., Escher, C., and Heinrich, M. (1997) Sesquiterpene lactone containing Mexican Indian medicinal plants and pure sesquiterpene lactones as potent inhibitors of transcription factor NF-kappaB. *FEBS Lett.* **402**, 85–90
46. Zacharis, C. K. (2009) Accelerating the quality control of pharmaceuticals using monolithic stationary phases: a review of recent HPLC applications. *J. Chromatogr. Sci.* **47**, 443–451
47. Gupta, V., Jain, A. D. K., Gill, N. S., and Guptan, K. (2012) Development and validation of HPLC method - a review. *IRJPAS*. **2**, 17–25
48. Galea, C., Mangelings, D., and Vander Heyden, Y. (2015) Characterization and classification of stationary phases in HPLC and SFC – a review. *Anal. Chim. Acta.* **886**, 1–15
49. Shrivastava, A., and Gupta, V. B. (2012) HPLC: Isocratic or Gradient Elution and Assessment of Linearity In Analytical Methods. *J. Adv. Res. Sci. Comput.* **3**, 12–20
50. Ian Freshney, R. (2016) *Culture of Animal Cells: A Manual of Basic Technique and Specialized Applications*, John Wiley & Sons
51. Somaiah, C., Kumar, A., Mawrie, D., Sharma, A., Patil, S. D., Bhattacharyya, J., Swaminathan, R., and Jaganathan, B. G. (2015) Collagen Promotes Higher

Adhesion, Survival and Proliferation of Mesenchymal Stem Cells. *PLoS One*. **10**, e0145068

52. Drexler, H. G., and Uphoff, C. C. (2002) Mycoplasma contamination of cell cultures: Incidence, sources, effects, detection, elimination, prevention. *Cytotechnology*. **39**, 75–90
53. Chen, T. R. (1977) In situ detection of mycoplasma contamination in cell cultures by fluorescent Hoechst 33258 stain. *Exp. Cell Res.* **104**, 255–262
54. Pulix, M., Lukashchuk, V., Smith, D. C., and Dickson, A. J. (2021) Molecular characterization of HEK293 cells as emerging versatile cell factories. *Curr. Opin. Biotechnol.* **71**, 18–24
55. Thomas, P., and Smart, T. G. (2005) HEK293 cell line: a vehicle for the expression of recombinant proteins. *J. Pharmacol. Toxicol. Methods*. **51**, 187–200
56. Bantscheff, M., Scholten, A., and Heck, A. J. R. (2009) Revealing promiscuous drug–target interactions by chemical proteomics. *Drug Discov. Today*. **14**, 1021–1029
57. Riss, T., Niles, A., Moravec, R., Karassina, N., and Vidugiriene, J. (2019) Cytotoxicity Assays: In Vitro Methods to Measure Dead Cells. in *Assay Guidance Manual* (Markossian, S., Grossman, A., Brimacombe, K., Arkin, M., Auld, D., Austin, C., Baell, J., Chung, T. D. Y., Coussens, N. P., Dahlin, J. L., Devanarayan, V., Foley, T. L., Glicksman, M., Gorshkov, K., Haas, J. V., Hall, M. D., Hoare, S., Inglese, J., Iversen, P. W., Kales, S. C., Lal-Nag, M., Li, Z., McGee, J., McManus, O., Riss, T., Saradjian, P., Sittampalam, G. S., Tarselli, M., Trask, O. J., Jr, Wang, Y., Weidner, J. R., Wildey, M. J., Wilson, K., Xia, M., and Xu, X. eds), Eli Lilly & Company and the National Center for Advancing Translational Sciences, Bethesda (MD)

58. Mosmann, T. (1983) Rapid colorimetric assay for cellular growth and survival: application to proliferation and cytotoxicity assays. *J. Immunol. Methods.* **65**, 55–63
59. Strober, W. (2001) Trypan blue exclusion test of cell viability. *Curr. Protoc. Immunol.* **Appendix 3**, Appendix 3B
60. Melouane, A., Ghanemi, A., Aubé, S., Yoshioka, M., and St-Amand, J. (2018) Differential gene expression analysis in ageing muscle and drug discovery perspectives. *Ageing Res. Rev.* **41**, 53–63
61. Chomczynski, P., and Sacchi, N. (2006) The single-step method of RNA isolation by acid guanidinium thiocyanate–phenol–chloroform extraction: twenty-something years on. *Nat. Protoc.* **1**, 581–585
62. Pawlowski, K., Kunze, R., De Vries, S., and Bisseling, T. (1994) Isolation of total, poly(A) and polysomal RNA from plant tissues. in *Plant Molecular Biology Manual* (Gelvin, S. B., and Schilperoort, R. A. eds), pp. 231–243, Springer Netherlands, Dordrecht
63. Shendure, J., and Ji, H. (2008) Next-generation DNA sequencing. *Nat. Biotechnol.* **26**, 1135–1145
64. Mardis, E. R. (2008) The impact of next-generation sequencing technology on genetics. *Trends Genet.* **24**, 133–141
65. Andrews, S., and Others (2010) FastQC: a quality control tool for high throughput sequence data
66. Anders, S., Pyl, P. T., and Huber, W. (2014) HTSeq—a Python framework to work with high-throughput sequencing data. *Bioinformatics.* **31**, 166–169

67. Love, M. I., Huber, W., and Anders, S. (2014) Moderated estimation of fold change and dispersion for RNA-seq data with DESeq2. *Genome Biol.* 15, 550
68. Goedhart, J., and Luijsterburg, M. S. (2020) VolcanoR is a web app for creating, exploring, labeling and sharing volcano plots. *Sci. Rep.* 10, 20560
69. Manku, G., and Culty, M. (2015) Dynamic changes in the expression of apoptosis-related genes in differentiating gonocytes and in seminomas. *Asian J. Androl.* 17, 403–414
70. Liu, T., Zhang, L., Joo, D., and Sun, S.-C. (2017) NF- κ B signaling in inflammation. *Signal Transduct Target Ther.* 2, 17023–17030
71. Flores-Romero, H., Hohorst, L., John, M., Albert, M.-C., King, L. E., Beckmann, L., Szabo, T., Hertlein, V., Luo, X., Villunger, A., Frenzel, L. P., Kashkar, H., and Garcia-Saez, A. J. (2022) BCL-2-family protein tBID can act as a BAX-like effector of apoptosis. *EMBO J.* 41, e108690
72. Voss, A. K., and Strasser, A. (2020) The essentials of developmental apoptosis. *F1000Res.* 10.12688/f1000research.21571.1
73. Korbecki, J., Maruszcwska, A., Bosiacki, M., Chlubek, D., and Baranowska-Bosiacka, I. (2022) The Potential Importance of CXCL1 in the Physiological State and in Noncancer Diseases of the Cardiovascular System, Respiratory System and Skin. *Int. J. Mol. Sci.* 10.3390/ijms24010205

VITA

After graduating from Texas A&M University, College Station, Texas in May of 2019 with a Bachelor of Science degree in Genetics, Jordan Monroe Sloan entered the Graduate School of Stephen F Austin State University, Nacogdoches, Texas in August 2021 and received the degree of Master of Science in May 2023.

Permanent Address: 4504 Scott Drive
Flower Mound, TX 75022

This thesis follows the style of the *Journal of Biological Chemistry*.

This thesis was typed by Jordan Monroe Sloan.